Simulation and Visualization of Fields and Energy Flows in Electric Circuits with Idealized Geometries

by

Mesrob I. Ohannessian

B.E. in Computer and Communications Engineering
American University of Beirut, 2002

Submitted to the Department of Civil and Environmental Engineering
in partial fulfillment of the requirements for the degree of

Master of Science

at the

MASSACHUSETTS INSTITUTE OF TECHNOLOGY

June 2005

Author .....
Department of Civil and Environmental Engineering
May 16, 2005

Certified by .....
John W. Belcher
Professor of Physics
Thesis Supervisor

Certified by .....
Steven R. Lerman
Professor of Civil and Environmental Engineering
Thesis Reader

Accepted by .....
Andrew J. Whittle
Chairman, Department Committee on Graduate Students

Simulation and Visualization of Fields and Energy Flows in Electric Circuits with Idealized Geometries

by

Mesrob I. Ohannessian

Submitted to the Department of Civil and Environmental Engineering
on May 16, 2005, in partial fulfillment of the
requirements for the degree of
Master of Science

Abstract

This thesis develops a method to simulate and visualize the fields and energy flows in electric circuits, using a simplified physical model based on an idealized geometry. The physical models combine and extend previously proposed models, to produce a rich array of interactive configurations of circuits. For example, both driven and undriven series RLC circuits can be simulated. The computation underlying the simulations is primarily the numerical solution of several first order differential equations and of a boundary value problem. The proposed visualization of these numerical results provide an appealing and physically meaningful representation of the fields and electromagnetic energy flows in these circuits.

Thesis Supervisor: John W. Belcher
Title: Professor of Physics

Thesis Reader: Steven R. Lerman
Title: Professor of Civil and Environmental Engineering

Acknowledgments

I would first like to thank Prof. John Belcher for proposing this problem – and others that shall remain unsung – and guiding me through it. However, it is for his contagious enthusiasm for and exemplary dedication to teaching that I look up to him, above all.

I thank Ralph Rabbat for introducing me to CECI. The rest of my journey I owe to the constant support of Prof. Steven Lerman. He has been, moreover, an invaluable advisor. I'm also grateful to the TEAL programming team – Phil Bailey, Mike Danziger, and Andrew McKinney – for being both marvelous coworkers and great friends. With the rest of the folks here – particularly Mark Bessette, Kirky Delong, Jud Harward, Pam Homsy, Maria Karatzas, Sen-Ben Liao and, of course, Meg Westlund – they created a unique synergy that gave CECI not just luster, but light.

More personally, I am grateful to Ghinwa Choueiter for being the best of friends. In her own way, she taught me to be more lucid, less naive, and much more human. I also would like to thank Prof. Rory O'Connor for his friendship and his pragmatic advice in countless situations.

Last but not least, I cannot thank my family enough for their love and sacrifice. They have spared nothing and endured much for me. They are my true blessing.

Contents

List of Figures

Chapter 1

Introduction

1.1 Motivation

In traditional introductory physics courses to electromagnetism, students are introduced to the concepts of electric charge, electric current, and electromagnetic fields and potentials, together with the equations governing the interaction of these quantities and their evolution in time. Then, using a subset of this rich array of principles, they are introduced to electric circuits. Certainly, the ability to analyze complex networks of electromagnetic components without referring to the underlying fields is useful, as the latter are often intractable by simple means. However, with this layer of abstraction, electric circuits lose part of their connection to basic physics.

The motivation of this thesis has been to bring out the electromagnetic nature of electric circuits and present it transparently to students in freshman electromagnetism. The medium through which we set to accomplish this goal are the simulation of simple electric circuits, and the visualization of the associated fields and the flow of electromagnetic energy.

For such a task, it is imperative to consider physical configurations simple enough to be amenable to analysis and interactive simulation, yet rich enough to provide a vast spectrum of experimentation. In this light, our work can be thought of as an extension of that by Heald [6, 7], the more rigorous analysis by Jackson [9], the communication by Clark [2], and the brief treatment by Majcen et al. [11].

The merit of the current work lies in the coherent amalgamation of some of the techniques presented in the above literature, coupled with the systematic construction of a physical model, the extension of existing physical models to include capacitance in addition to emf, resistance and inductance, and, last but not least, the introduction of a meaningful visualization method for the flow of electromagnetic energy.

It is worth noting that our simulation is implemented in a software package pre-equipped with techniques for field visualization, such as streamlines and texture based vector field representations in the style of line integral convolution (LIC)[1], [12]. These augment the educational value of the simulation and make it more appealing.

We hope that the tool we have developed will indeed help students perceive electric circuits as true physical phenomena, rather than mere mathematical equations.

1.2 Scope and Organization

Chap. 2 defines and characterizes the circuit to be a thin cylindrical shell of infinite height, with which physical properties are associated. The numerical computation of circuit quantities is outlined. Chap. 3 studies the fields associated with the circuit. The magnetic field and the electric field, in two components, are derived and their numerical computation is detailed. Chap. 4 uses the field quantities to obtain the electromagnetic energy density in space, as well as its flow in time. This flow is quantized, and an effective visualization is obtained. Chap. 5 concludes the thesis with some examples.

Chapter 2

Circuit

In this chapter we describe the conceptual construction of an idealized geometry electric circuit. In Sec. 2.1 we define the geometrical setting of the problem as a cylindrical shell of infinite height. In Sec. 2.2 we move on to ascribe physical properties to the shell. In Sec. 2.3 we explain certain assumptions crucial for subsequent development. Finally, in Sec. 2.4 we complete the description by coalescing the development into a classical circuit model, directly amenable to simulation.

2.1 General Geometry

The choice of a geometry for the problem of analyzing and visualizing the fields and the energy flow associated with an electric circuit is chiefly motivated by the potential tractability of the problem in terms of both analysis and numerical computation. This thesis adopts an infinite height cylindrical shell, of radius a and negligible thickness $\delta \ll a$, as the support of the electric circuit, as shown in Fig. 2-1(a). Chap. 3 provides the bulk of justification for selecting this geometry. Infinite height, for instance, together with only angularly varying physical properties, as presented in Sec. 2.2, provide invariance under axial translation. This and cylindrical shape confine the electric field to two dimensions and the magnetic field to one, rather than the usual three. Cylindrical shape also allows us to conveniently specify the boundary condition when solving the partial differential equation for the electrostatic potential.

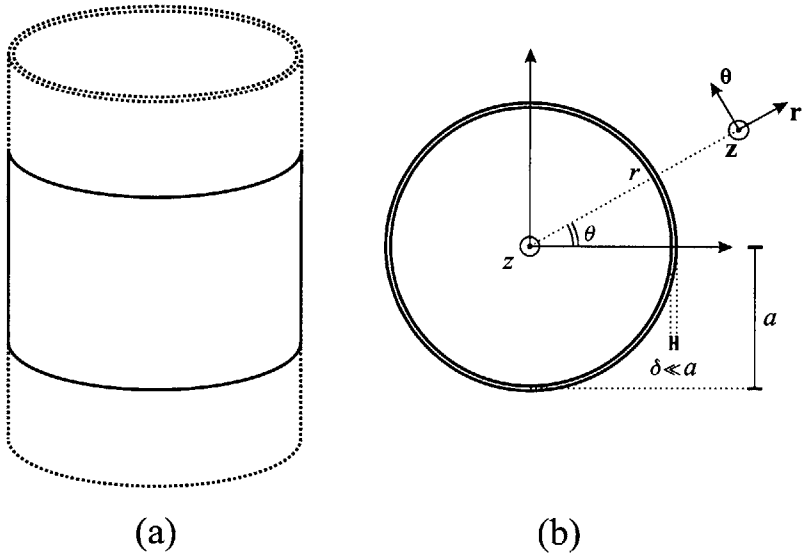

Figure 2-1: Our electric circuit is an infinite-height cylindrical shell, of radius a and negligible thickness $\delta \ll a$ (a), with which we associate a cylindrical coordinate system (b).

With this geometry it is most convenient to work in a system of cylindrical coordinates (r, θ, z), where the z-axis coincides with that of the cylindrical shell of the circuit, as shown in Fig. 2-1(b).

2.2 Physical Properties

To construct the equivalent of an electric circuit on our cylindrical shell, we need to attribute physical properties to the material. In this section, we study all properties that will allow us to build resistors, batteries and capacitors. The cylinder itself will act as an inductor. We start with some introductory analysis. This will introduce our framework and demonstrate how the conventional notions of resistance and current must be naturally replaced with normalized equivalents.

Without loss of generality, we first consider an isolated section of the cylindrical shell, which we make of finite length h, and postpone studying the $h \to \infty$ limiting behavior and its consequences to later. The section extends between $\theta = 0$ and $\theta = \theta^\star$, which we refer to as the *extremities* of the section.

The cut surfaces at the extremities are planes normal to $\hat{\boldsymbol{\theta}}$. We choose the resistivity $\rho(\theta)$ to be a function of angle, but uniform in the radial and axial directions. Our task is to find the resistance R of this section. The whole configuration is shown in Figure 2-2. We start by applying an external emf source, which gives $V(\theta^\star) = -\mathcal{E}$, if $V(0) = 0$ is our reference. This gives rise to a current I, from which we obtain the resistance of the section $R_S = \left|\frac{\mathcal{E}}{I}\right|$.

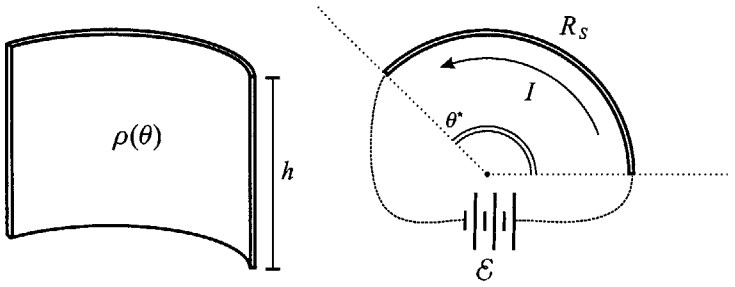

Figure 2-2: Configuration for the calculation of the resistance of a section of the cylindrical shell of height h and arc length $\theta^\star$ and of resistivity $\rho(\theta)$.

We restrict our consideration to the case of steady current, i.e. after the system stabilizes and there is no charge accumulation or dispersion at any point in the conductor. This state is reached very quickly, as we justify in Sec. 2.3. In this situation, we can write the continuity equation as,

$$\boldsymbol{\nabla} \cdot \mathbf{J} = -\frac{\partial \rho_v}{\partial t} = 0, \tag{2.1}$$

where ρ_v is the volume charge density. Notice that, by the divergence theorem, this implies that the total current flowing out of a closed region encircling any part of the section, and possibly empty space surrounding it, is zero. One consequence of this is that the current I computed by integrating $\mathbf{J}$ over any complete cross-section will be the same. This follows from taking a closed surface that contains both the given cross-section and an extremity cut surface, and which closes outside of the conductor. Since there is no current outside, the current through the arbitrary cross-section is the same as the one going into, or out of, the extremity.

Now, we need to find the electric field $\mathbf{E}$ inside the section, from which we can obtain the current density $\mathbf{J}$ from Ohm's law,

$$\mathbf{E} = \rho\mathbf{J}, \tag{2.2}$$

we then integrate $\mathbf{J}$ over a cross-section to obtain I.

Other than the boundary conditions imposed on the potential at the extremities, we require that no current flows across the conductor, except through the extremities themselves. This can be translated into the following *no-leak* requirements:

$$\begin{aligned} \mathbf{E}\cdot\mathbf{r} &= 0 \text{when } r = a \pm \frac{\delta}{2}, \quad 0 < \theta < \theta^\star, \quad \text{and } -\frac{h}{2} < z < \frac{h}{2} \\ \mathbf{E}\cdot\mathbf{z} &= 0 \text{when } a - \frac{\delta}{2} < r < a + \frac{\delta}{2}, \quad 0 < \theta < \theta^\star, \quad \text{and } z = \pm\frac{h}{2}. \end{aligned} \tag{2.3}$$

However, the problem is an electrostatic one, and thus we can write $\mathbf{E} = -\boldsymbol{\nabla}V = -\frac{\partial V}{\partial r}\hat{\mathbf{r}} - \frac{1}{r}\frac{\partial V}{\partial \theta}\hat{\boldsymbol{\theta}} - \frac{\partial V}{\partial z}\hat{\mathbf{z}}$. The requirements in Eq. (2.3) transform into boundary conditions on the potential: $\frac{\partial V}{\partial r} = 0$ and $\frac{\partial V}{\partial z} = 0$, on the appropriate faces of the section. However, if we can find a valid solution for the potential which satisfies the boundary conditions at the extremities, and which is independent of the radial and axial components *everywhere within the section*, then these no-leak requirements will be automatically satisfied, and we would have found *the* solution, based on the uniqueness theorem.

What is the equation that the potential must satisfy within the section? If the material had uniform resistivity, Laplace's equation would apply. However, that is not the case, and we have instead the following:

$$\begin{aligned} \boldsymbol{\nabla}\cdot\mathbf{E} &= \boldsymbol{\nabla}\cdot(\rho\mathbf{J}) \\ -\nabla^2 V &= \rho\underbrace{\boldsymbol{\nabla}\cdot\mathbf{J}}_{0} + \underbrace{\mathbf{J}}_{\mathbf{E}/\rho}\cdot\boldsymbol{\nabla}\rho \\ -\nabla^2 V &= -\frac{1}{\rho}\boldsymbol{\nabla}V\cdot\boldsymbol{\nabla}\rho \end{aligned} \tag{2.4}$$

Let us now, as we mentioned, search for solutions where the potential is a function of θ alone. This restriction gives us $\nabla^2 V = \frac{1}{r^2}\frac{\partial^2 V}{\partial \theta^2}$, $\boldsymbol{\nabla} V = \frac{1}{r}\frac{\partial V}{\partial \theta}$ and $\boldsymbol{\nabla}\rho = \frac{1}{r}\frac{\partial \rho}{\partial \theta}$, and we can write

$$\frac{\partial^2 V}{\partial \theta^2} = \frac{1}{\rho}\frac{\partial V}{\partial \theta}\frac{\partial \rho}{\partial \theta}, \tag{2.5}$$

which admits solutions of the form $\frac{\partial V}{\partial \theta} = K\rho$, or equivalently

$$V(\theta) = K\int_0^\theta \rho(\theta')\mathrm{d}\theta' + \underbrace{V(0)}_{0} \tag{2.6}$$

This equation satsifies the boundary condition at $\theta = 0$, and we can find a suitable value for K to satisfy that at $\theta = \theta^\star$:

$$K = \frac{\overbrace{V(\theta^\star)}^{-\mathcal{E}}}{\int_0^{\theta^\star}\rho(\theta')\mathrm{d}\theta'}. \tag{2.7}$$

Since the resulting solution is in accord with all boundary conditions, be they the potential at the extremities or the no-leak requirements, it is the only solution, by the uniqueness theorem. The electric field and the current density are given by:

$$\mathbf{E} = -\boldsymbol{\nabla} V = -\frac{1}{r}\frac{\partial V}{\partial \theta} = -\frac{K\rho}{r}\hat{\boldsymbol{\theta}}, \tag{2.8}$$

$$\mathbf{J} = \mathbf{E}/\rho = -\frac{K}{r}\hat{\boldsymbol{\theta}}. \tag{2.9}$$

To calculate the current, let us consider any cross-section normal to $\hat{\boldsymbol{\theta}}$:

$$\begin{aligned} I &= \iint \mathbf{J}\cdot\mathrm{d}\mathbf{s} = \int_{-h/2}^{h/2}\int_{a-\delta/2}^{a+\delta/2}\mathbf{J}\cdot\hat{\boldsymbol{\theta}}\mathrm{d}r\mathrm{d}z \\ &= \int_{-h/2}^{h/2}\int_{a-\delta/2}^{a+\delta/2} -\frac{K}{r}\mathrm{d}r\mathrm{d}z \\ &= -Kh\ln\left(\frac{a+\delta/2}{a-\delta/2}\right) \\ &\approx -Kh\frac{\delta}{a} \\ &= \frac{\mathcal{E}h\delta}{a\int_0^{\theta^\star}\rho(\theta')\mathrm{d}\theta'}. \end{aligned} \tag{2.10}$$

For the approximation step, we have used the first term of the Maclaurin expansion $\ln\left(\frac{1+\epsilon}{1-\epsilon}\right) = 2\epsilon + \frac{2}{3}\epsilon^3 + \frac{2}{5}\epsilon^5 + \ldots$ valid for $-1 < \epsilon < 1$, which applies to $\epsilon = \delta/2a$, since we have taken $\delta \ll a$. Finally, the expression for the current gives us the resistance of the section

$$R_S = \left|\frac{\mathcal{E}}{I}\right| = \frac{a\int_0^{\theta^\star}\rho(\theta')\mathrm{d}\theta'}{h\delta} \qquad \Omega, \tag{2.11}$$

which makes it clear that

$$\lim_{h\to\infty} R_S = 0,$$

since, although δ is small compared to a, the $\frac{a}{\delta}$ ratio is still finite. Consequently, for any non-zero potential difference the current is infinite, or alternatively any finite current will result in a zero potential difference. This shows that we need to modify the quantities we are to work with, in order to do some meaningful analysis.

2.2.1 Current and Charge

We first start by restricting the integration in Eq. (2.10) to a unit length. The resulting quantity is the current per unit length, which we denote by κ, expressed in amperes per meter (A/m),

$$\kappa = \iint \mathbf{J}\cdot\mathrm{d}\mathbf{s} = \int_{-1/2}^{1/2}\int_{a-\delta/2}^{a+\delta/2} \mathbf{J}\cdot\hat{\boldsymbol{\theta}}\,\mathrm{d}r\mathrm{d}z \tag{2.12}$$

The current convention is implicitly defined in Eq. (2.12) to be positive in the counterclockwise, or $\hat{\boldsymbol{\theta}}$, direction. For the resistive case, we have

$$\kappa = \frac{\mathcal{E}\delta}{a\int_0^{\theta^\star}\rho(\theta')\mathrm{d}\theta'} \qquad \mathrm{A/m}. \tag{2.13}$$

Note that κ is finite despite the fact that the total current in the ring is infinite. Moreover, by virtue of the symmetry of the problem, we know that we obtain the same value of κ, over *any* unit length integration interval. We will preserve this symmetry in general, by making all properties of the cylindrical shell invariant under axial translation.

The notion of current per unit length extends directly to charge, and we can define the charge per unit length that passes through a cross-section during a time T, λ, expressed in coulombs per meter (C/m), based on the relationship:

$$\lambda = \int_T \kappa dt \qquad \text{C/m}. \tag{2.14}$$

We now attempt to relate the current density directly to the current. We write

$$\mathbf{J} = J_r(r,\theta,z)\hat{\mathbf{r}} + J_\theta(r,\theta,z)\hat{\boldsymbol{\theta}} + J_z(r,\theta,z)\hat{\mathbf{z}}$$

First, we know that an axial component and axial dependence are prohibited by symmetry, thus $J_z = 0$, and neither J_r nor J_θ depend on z. Next, the fact that the current is steady makes $\mathbf{J}$ a continuous and differentiable function within the cylindrical shell. Now, since δ is very small, we can argue that $J_\theta(r,\theta)$ has almost the same value for any r, and thus drop that index completely. We can then write

$$\iint \mathbf{J}\cdot \mathrm{ds} = \int_{-1/2}^{1/2}\int_{a-\delta/2}^{a+\delta/2} \mathbf{J}\cdot\hat{\boldsymbol{\theta}}\, \mathrm{d}r\mathrm{d}z = \delta J_\theta(\theta).$$

Notice that this is tantamount to invoking the mean value theorem, and taking the limit when $\delta \to 0$. Also, by Eq. (2.12), the above is simply κ. Since the latter is not a function of θ, J_θ cannot be a function of θ, and thus $\kappa = \delta J_\theta$.

This relates J_θ to κ, but we still have J_r to deal with. However, when computing current flow through an arbitrary unit height cut surface, the above tells us that J_θ will contribute exactly κ, as it is constant, and thus needs only to be multiplied by the $\hat{\boldsymbol{\theta}}$ projection of the surface, which is always δ. The component due to J_r is zero, and since this is valid for any such surface, we deduce that so is J_r itself. We can now state our approximation precisely:

$$\mathbf{J} = \frac{\kappa}{\delta}\,\hat{\boldsymbol{\theta}}. \tag{2.15}$$

2.2.2 Resistance

We now modify the usual definition of resistance to obtain R, the resistance per unit length, expressed in ohm-meters ($\Omega\,\mathrm{m}$):

$$\begin{aligned} R = \left|\frac{\mathcal{E}}{\kappa}\right| &= a\int_0^{\theta^\star} \frac{1}{\delta}\rho(\theta')\mathrm{d}\theta' \qquad \Omega\,\mathrm{m}. \\ &= a\int_0^{\theta^\star} \rho_\delta(\theta')\mathrm{d}\theta' \qquad \Omega\,\mathrm{m}. \end{aligned} \tag{2.16}$$

The reason why the distance unit is in the numerator is seen by analogy to resistors in parallel. Indeed, since there is no current flowing axially, each unit-height strip within the shell section shown in Fig. 2-2 acts as an independent resistor, in parallel with all others. From this we can also see how the resistance of the section goes to zero in the limit, as it becomes the inverse of a sum of infinitely many non-zero inverses: $R_S = \frac{1}{1/R+\ldots+1/R}$. Finally, note that Eq. (2.16) makes explicit use of the shell thickness δ. However, it is convenient to specify this quantity only implicitly. This is the reason why we absorb it into the resistivity, and denote the resulting quantity by $\rho_\delta(\theta)$, expressed in ohms (Ω).

Using Ohm's law, Eq. (2.2) and the approximation of the current density, Eq. (2.15), we can express the electric field in resistive sections of the shell as follows:

$$\begin{aligned} \mathbf{E} &= \rho(\theta)\mathbf{J} \\ &= \rho(\theta)\frac{\kappa}{\delta}\hat{\boldsymbol{\theta}} \\ &= \rho_\delta(\theta)\kappa\hat{\boldsymbol{\theta}}. \end{aligned} \tag{2.17}$$

As the isomorphism with the regular quantities is close to perfect, we hereafter refer to κ as *the* current, to λ as *the* charge and to R as *the* resistance, for brevity, and revert to the exact terminology when clarity requires.

2.2.3 Electromotive Force

Thus far, we have taken all potential differences to be due to an external source of emf. However, this alters our idealized geometry, and the analysis of fields and energy flow is no longer tractable. As an alternative, we confer to the cylindrical shell an inherent electromotive property, that exercises a force $\mathbf{f}$ per unit charge in the angular direction, expressed in newtons per coulomb (N/C), or volts per meter (V/m). Similarly to resistivity, we choose $\mathbf{f}$ to be a function of angle, uniform in the radial and axial directions:

$$\mathbf{f} = f(\theta)\hat{\boldsymbol{\theta}} \qquad \text{V/m.} \tag{2.18}$$

After a very short transient acceleration, an electric field $\mathbf{E}$ which exactly counters $\mathbf{f}$ is established, for reasons we give in Sec. 2.3. The outcome is that all charges end up moving at constant drift velocity, resulting in a steady current κ. We have,

$$\mathbf{E} = -f(\theta)\hat{\boldsymbol{\theta}}. \tag{2.19}$$

2.2.4 Capacitance

Capacitors are obtained by introducing a gap within the cylinderical shell, and placing perfectly conducting plates across the gap. As illustrated in Fig. 2-3, the plates have a finite width ℓ, and a separation of $d = a\Delta\theta$. By analogy to capacitance, which is the geometric proportionality constant between potential difference and charge, we define the per unit length capacitance C of the gap, expressed in farads per meter (F/m), as follows:

$$C = \frac{\lambda}{\Delta V} \qquad \text{F/m.} \tag{2.20}$$

In order not to distort the cylindrical geometry, we assume that $\ell \ll a$. Nevertheless, we impose $\delta < \ell$ and d small enough. The first restriction means that charge associated with the capacitor will be approximately evenly distributed over the plates, $+\lambda$ on one and $-\lambda$ on the other.

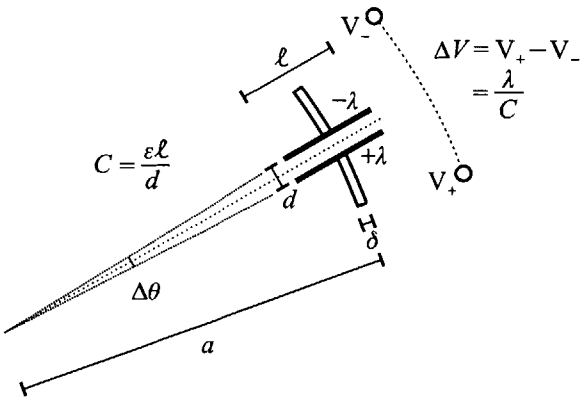

Figure 2-3: A capacitive gap, formed by infinite-height parallel plates of width ℓ and separation d.

The second restriction allows us to consider the plates themselves to be infinite planes for the purpose of approximating the electric field between them with a convenient expression. We thus have:

$$C = \frac{\epsilon \ell}{d}, \tag{2.21}$$

$$\mathbf{E} = \frac{\lambda}{\epsilon \ell} \hat{\boldsymbol{\theta}}. \tag{2.22}$$

Both expressions follow immediately from those of the regular parallel plate capacitor, which has capacitance $\epsilon S/d$ and electric field magnitude $Q/(\epsilon S)$. In order to be consistent with our current convention, positive current deposits charges, thus yields a positive rate of change, on the first plate, in the counterclockwise direction, whence the $+\lambda$ label given to that plate in Fig. 2-3.

Note that Eq. (2.22) was derived in a static context. We now justify the fact that subsequently we consider it to be the total electric field in capacitive regions, in general. In Sec. 3.2 we show that the "nonstatic" component of the electric field is in the angular direction. In this light, we can reverse the causality of the argument, and start with an electric field $\mathbf{E} = E\hat{\boldsymbol{\theta}}$ in the angular direction. Then, as long as field variations are not too fast, as assumed in Sec. 2.3, the charge closely follows its otherwise electrostatic distribution, i.e. $\lambda = \ell \epsilon E$. This completes our justification.

Sometimes it is desirable to have a capacitor that is not very localized, in order to avoid an electrostatic potential that varies too rapidly with θ (cf. Sec. 3.2.3, discretization of the surface potential). To circumvent the requirement of d being small, we can stack several capacitors back to back, as shown in Fig. 2-4. If the resulting capacitive set is formed of n such gaps, and if all plates have width ℓ and separation d, then the electric field is still given by Eq. (2.22), the potential difference over each gap is $\Delta V/n$, and the capacitance is divided by n compared to Eq. (2.21):

$$C = \frac{\epsilon \ell}{nd}. \tag{2.23}$$

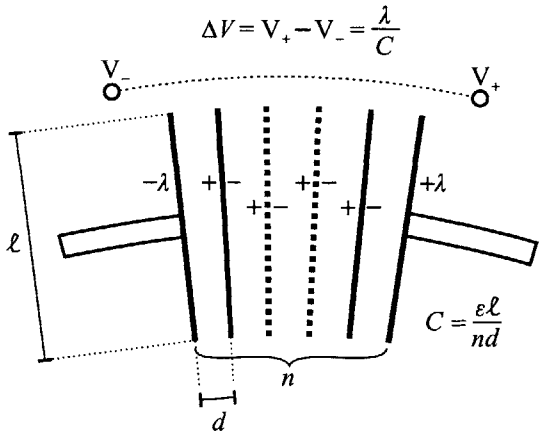

Figure 2-4: A capacitive set formed by n capacitive gaps placed back to back, acting as capacitors in series.

2.2.5 Inductance

We associate with a closed current loop $\mathcal{C}$, the self-flux Φ across its surface $\mathcal{S}$, expressed in webers,

$$\Phi = \iint_S \mathbf{B} \cdot \mathrm{ds} \qquad \mathrm{Wb}, \tag{2.24}$$

where $\mathbf{B}$ is the magnetic field, in teslas (T). In Eq. (2.24), we can replace $\mathcal{S}$ by any other surface $\mathcal{S}'$, bounded by $\mathcal{C}$. To see this, we use the divergence theorem on the closed surface formed by $\mathcal{S}$ and $\mathcal{S}'$:

$$\iint_{S+S'} \mathbf{B} \cdot \mathrm{ds} = \iiint_{\mathcal{V}} \nabla \times \mathbf{B} \, \mathrm{d}v$$
$$\iint_{S} \mathbf{B} \cdot \mathrm{ds} - \iint_{S'} \mathbf{B} \cdot \mathrm{ds} = 0, \tag{2.25}$$

where the changing surface normal is the reason behind the closed surface integral being the difference of individual surface integrals.

In the general case, by the Biot-Savart law, the magnetic field of $\mathcal{C}$ at every point is the product of the current with a vector function which is purely geometric in nature. Let's write this as $\mathbf{B} = I\mathbf{g}$. By integrating, we obtain $\Phi = I \iint \mathbf{g} \cdot \mathrm{ds}$. This yields a simple proportionality relationship between the self-flux Φ and the current I. The constant of proportionality is the self-inductance of $\mathcal{C}$, expressed in henries (H),

$$L_{\mathcal{C}} = \frac{\Phi}{I} = \iint \mathbf{g} \cdot \mathrm{ds} \qquad \mathrm{H}.$$

In our case, we treat the cylinder itself as a current loop. As we will see in Sec. 3.1, $\mathbf{B}$ is the product of the current per unit length κ with a geometric vector function, $\mathbf{B} = \kappa\mathbf{g}'$. By analogy to the current loop, we define the self-inductance of the cylinder as follows, expressed in henry-meters,

$$L = \frac{\Phi}{\kappa} = \iint \mathbf{g}' \cdot \mathrm{ds} \qquad \mathrm{H\,m}. \tag{2.26}$$

2.3 Assumptions

One of the assumptions underlying most of the presentation is the fact that the current is steady. When a current κ flows through the cylinder, we assume that its magnitude is the same everywhere. In general, the surface charge distribution, which we see analytically in Sec. 3.2.2, has an important regulatory role – see for instance [9]. Here we present intuitive arguments, justifying the assumption depending on the physical properties of various sections of the cylinder.

(a) Within perfectly conducting sections, if the current is not uniform, then charge builds up in such a way that an electric field is induced that regulates the current and makes it uniform For example, if more current flows into a given closed region than out of it, then positive charge accumulates within that region. The electric field is then outward from the region, which assists the outgoing current and impedes the incoming. This effect persists until there is no electric field, i.e. there is no net charge buildup. When κ is a time variable, we assume the speed of this stabilization to be much larger than any variation in κ.

(b) Within electromotive sections, a force $\mathbf{f}$ is experienced per unit charge. This, however, accelerates the charges, which yields non-uniform current, since the velocity of a charge going out of a closed region is greater than its velcotiy when going into the region. According to the same principle as in (a), charges assume a distribution such as an electric field $\mathbf{E}$, opposing $\mathbf{f}$, is induced. However, unlike (a), $\mathbf{E}$ does not eventually disappear, because it grows in magnitude until it exactly balances $\mathbf{f}$, and keeps that magintude since then there will be no net force on charges, and hence no acceleration and no buildup. Note that since charges move in the direction of $\mathbf{f}$, $\mathbf{E}$ opposes current flow in these sections.

(c) Within resistive sections, charges effectively experience a force opposing their direction of motion, and proportional to their drift velocity, or, equivalently, the current density, say $-\rho\mathbf{J}$. As a result, similarly to (b), charges are distributed in such a way that an electric field $\mathbf{E}$, exactly opposing $-\rho\mathbf{J}$ is induced. Here, however, since the force itself is against the current flow, $\mathbf{E}$ is in the direction of current flow.

(d) Within capacitive sections, there is no real current flow, because of the gaps. However, it is possible to show that the displacement current within the gaps, say κ_d, is exactly equal to κ. Since the effective current density in the Maxwell equations is the sum of actual and displacement current densities, we can simplify our notation by assuming that current does flow in capacitive sections, and is equal to the displacement current, and by that token, to the actual current.

To show the equivalence, we use Eq. (2.22) to get $\lambda = \ell\epsilon\mathbf{E}\cdot\hat{\boldsymbol{\theta}}$. This allows us to write:

$$\begin{aligned}\kappa &= \frac{\mathrm{d}\lambda}{\mathrm{d}t} \\ &= \ell\frac{\partial\epsilon\mathbf{E}}{\partial t}\cdot\hat{\boldsymbol{\theta}} \\ &= \int_{\text{gap}}\frac{\partial\epsilon\mathbf{E}}{\partial t}\cdot\hat{\boldsymbol{\theta}}\mathrm{d}r \\ &= \kappa_d.\end{aligned}$$

We will always neglect the displacement current everywhere, except within capacitive gaps, as we have seen above. The tacit assumption behind this is the *magnetoquasistatics* approximation. What we mean by this is that the variation in the electric field are generally small enough to be neglected in the magnetic curl equation

$$\begin{aligned}\frac{1}{\mu}\boldsymbol{\nabla}\times\mathbf{B} &= \mathbf{J}+\frac{\partial\epsilon\mathbf{E}}{\partial t} \\ &\approx \mathbf{J}.\end{aligned} \tag{2.27}$$

This is another way of saying that the contribution of the actual current density overshadows that of the displacement current density, which we can think of as an "error" quantity. From this perspective, our assumption can be quantitavely justified after a simulation, which amounts to a first approximation, by computing the error and making sure that it remains small. Note that the assumption also effectively decouples magnetic fields from electric fields, and thus forbids electromagnetic waves. Therefore, for it to be a valid approximation, field changes must propagate fast enough across the circuit, that is we must have

$$c \gg \frac{a}{\tau},$$

where τ is the time scale of the operation of the circuit, and quantifies the rate of change of the electromagnetic sources, i.e. charges and current.

Finally we come to our last assumption. Recall how current flow in resistive sections is made possible by a charge distribution which induces an electric field exactly countering the resistive force. However, since charge experiences force due to either an electric field or motion relative to a magnetic field, the latter can assist in balancing out the resistive force $-\rho\mathbf{J}$, by contributing $\mathbf{v} \times \mathbf{B}$ per unit charge, based on the force law. This means that a uniform current is obtained when $\mathbf{E}$ is induced such that:

$$\mathbf{E} + \mathbf{v} \times \mathbf{B} = \rho\mathbf{J}. \tag{2.28}$$

This can be thought of as a generalized Ohm's law, and is only needed when the charges move at large velocities relative to the magnetic field. For our purpose, the simple Ohm's law given by Eq. (2.2) is sufficient.

2.4 Analysis

2.4.1 Equivalent Circuit

Let us first combine the total electric field due to all properties of the cylindrical shell. When a section of the shell has both resistive and electromotive properties, there will be two components to the electric field, one that counters $\mathbf{f}$ and thus works to halt the acceleration of charges, and another that works towards maintaining current in the resistive medium. Therefore, we can combine Eq. (2.17) and Eq. (2.19) additively.

Capacitive sections do not overlap with these sections, and thus have their electric field given by Eq. (2.22). Assume we have distinct capacitive sections indexed by i, such as the width of the plates in each such section is a constant ℓ_i. For convenience of expression, let $\mathscr{I}_i(\theta)$ be indicator functions that are 1 when θ is within capacitive section i, and 0 otherwise. Finally, uniform current implies that all capacitive regions carry the same amount of charge, λ.

All parts of the the circuit that do not have resistive, electromotive or capacitive properties assumed to be perfect conductors. As such, the electric field is exactly zero within these connective sections.

The combination of these gives the electric field everywhere within the circuit:

$$\mathbf{E} = \left[\rho_\delta(\theta)\kappa - f(\theta) + \sum_i \mathscr{I}_i(\theta)\frac{\lambda}{\epsilon\ell_i}\right]\hat{\boldsymbol{\theta}}. \tag{2.29}$$

Using Stoke's theorem, we can write the circuit integral of the electric field, over a path coinciding with a normal cross-section of the cylinder, as follows:

$$\begin{aligned}
\oint \mathbf{E}\cdot\mathrm{d}\boldsymbol{\ell} &= \iint \boldsymbol{\nabla}\times\mathbf{E}\cdot\mathrm{ds} \\
\oint \left[\rho_\delta(\theta)\kappa - f(\theta) + \sum_i \mathscr{I}_i(\theta)\frac{\lambda}{\epsilon\ell_i}\right] a\mathrm{d}\theta &= \iint -\frac{\partial\mathbf{B}}{\partial t}\cdot\mathrm{ds} \\
\left(\oint \rho_\delta(\theta)a\mathrm{d}\theta\right)\kappa - \oint f(\theta)a\mathrm{d}\theta + \left(\oint \sum_i \frac{\mathscr{I}_i(\theta)}{\epsilon\ell_i}a\mathrm{d}\theta\right)\lambda &= -\frac{\mathrm{d}}{\mathrm{d}t}\iint \mathbf{B}\cdot\mathrm{ds} \\
R_\circ\kappa - \mathcal{E}_\circ + \frac{1}{C_\circ}\lambda &= -\frac{\mathrm{d}}{\mathrm{d}t}\Phi.
\end{aligned} \tag{2.30}$$

It is important to note that the extraction of the partial differentiation out of the integral as ordinary differentiation, in the third step above, is only made possible due to the stationarity and fixed geometry of the integration surface. If this were not the case, we should have subtracted the components of $\frac{\mathrm{d}}{\mathrm{d}t}\iint \mathbf{B}\cdot\mathrm{ds}$, which are due to motion and geometric variation, in order to isolate $\iint \frac{\partial\mathbf{B}}{\partial t}\cdot\mathrm{ds}$.

Using Eq. (2.14) and Eq. (2.26), we can write Eq. (2.30) solely in terms of the current κ. We refer to the resulting integro-differential equation as the *circuit equation*, as it governs the circuit's evolution in time:

$$R_\circ\kappa - \mathcal{E}_\circ + \frac{1}{C_\circ}\int \kappa\mathrm{d}t = -L\frac{\mathrm{d}\kappa}{\mathrm{d}t}. \tag{2.31}$$

Notice how, by deriving Eq. (2.31), we have lumped all properties together as properties of the circuit as a whole, rather than distributed properties, at every point of the shell. These are *circuit resistance*:

$$R_\circ = \oint \rho_\delta(\theta)a\mathrm{d}\theta \qquad \Omega\,\mathrm{m}, \tag{2.32}$$

circuit emf,

$$\mathcal{E}_\circ = \oint f(\theta) a \mathrm{d}\theta \qquad \mathrm{V}. \tag{2.33}$$

and *circuit capacitance*:

$$C_\circ = \left[\oint \sum_i \frac{\mathscr{I}_i(\theta)}{\epsilon \ell_i} a \mathrm{d}\theta \right]^{-1} \qquad \mathrm{F\,m}. \tag{2.34}$$

At this point, we recognize that we can work with an equivalent circuit with lumped components as illustrated in Fig. 2-5. Henceforth, we adopt this conceptual picture.

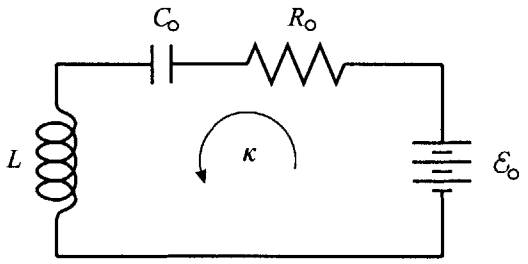

Figure 2-5: Lumped component circuit, equivalent to the actual circuit for the purposes of analysis.

2.4.2 Discrete Component Model

In order to have a manageable simulation, it is convenient to specialize the largely continuous model described so far to a situation more reminiscent of discrete components. As we shall see in Sec. 3.2.2 and Sec. 4.2, this also allows us to perform surface scalar potential and energy calculations in a straightforward manner.

To obtain discrete *resistors*, we have to restrict ourselves to sections of homogeneous resistivity. Similarly, for discrete emf sources, which we refer to as *batteries*, we need homogeneous emf in each section. Eq. (2.32) and Eq. (2.33) show that lumping these results in the familiar additive series formulas. Let us denote by $\Delta\theta_{\mathcal{C}}$ the extent of component $\mathcal{C}$ and by $\theta^\star_{\mathcal{C}}$ its starting angle, and let us have a suitable index for each type of component ($\mathcal{I}_R$, $\mathcal{I}_\mathcal{E}$ and $\mathcal{I}_C$ for resitors, batteries and capacitors respectively).

Using the component's name for its lumped property, we have, in summary:

$$R_i = \int_{\theta^\star_{R_i}}^{\theta^\star_{R_i}+\Delta\theta_{R_i}} \rho_{\delta i} a \mathrm{d}\theta = \rho_{\delta i}(a\Delta\theta_{R_i}), \qquad \text{with} \quad R_\circ = \sum_{i\in\mathcal{I}_R} R_i \qquad \text{and} \tag{2.35}$$

$$\mathcal{E}_i = \int_{\theta^\star_{\mathcal{E}_i}}^{\theta^\star_{\mathcal{E}_i}+\Delta\theta_{\mathcal{E}_i}} f_i a \mathrm{d}\theta = (a\Delta\theta_{\mathcal{E}_i}) f_i, \qquad \text{with} \quad \mathcal{E}_\circ = \sum_{i\in\mathcal{I}_\mathcal{E}} \mathcal{E}_i. \tag{2.36}$$

As for *capacitors*, notice how our presentation of capacitive sections already allows us to treat them as discrete components. With Eq. (2.34), we have the familiar series formula for capacitors:

$$C_i = \left[\int_{\mathscr{I}_i(\theta)=1} \frac{1}{\epsilon\ell_i} a \mathrm{d}\theta\right]^{-1} = (\epsilon\ell_i)/(a\Delta\theta_{C_i}), \qquad \text{with} \quad C_\circ = \left(\sum_{i\in\mathcal{I}_C} i\frac{1}{C_i}\right)^{-1}. \tag{2.37}$$

Finally, within the extent of each component $\mathcal{C}$ in this discrete component model the electric field is a constant of the form $\mathbf{E}_\mathcal{C} = E_\mathcal{C}\hat{\boldsymbol{\theta}}$. Using the lumped properties for each type of component, given by Eq. (2.35), Eq. (2.36) and Eq. (2.37), we have

$$E_{R_i} = \rho_{\delta i}\kappa = R_i\kappa/(a\Delta\theta_{R_i}), \tag{2.38}$$

$$E_{\mathcal{E}_i} = -f_i = -\mathcal{E}_i/(a\Delta\theta_{\mathcal{E}_i}), \tag{2.39}$$

$$\text{and} \quad E_{C_i} = \frac{\lambda}{\epsilon\ell_i} = \frac{\lambda}{C_i}/(a\Delta\theta_{C_i}). \tag{2.40}$$

2.4.3 Numerical Computation

The circuit equation, Eq. (2.31), degenerates when one or more physical property is missing. We treat each of the four cases (RLC, RL, RC, and R-only) independently, in order to unambiguously define all quantities in these degenerate situations.

We assume that a solver for systems of first order differential equations, e.g. Euler or Runge-Kutta, is available. The independent variable of all equations is time. As for the dependent variables, we show that the RLC and LC cases integrate both charge and current, the RL case integrates just current, the RC case just charge, and the R case does not require integration.

For each case, we also explain what quantity can be set by the simulation user, and what cannot. The derivative of the current is a quantity we need when evaluating electromagnetic fields in Chap. 3, even when not needed for integration. Therefore, we explicitly express it in all cases.

RLC Case

In the general case, the circuit equation is second order. It can be split into two first order equations in the natural way, one in charge and one in current:

$$\begin{aligned} \frac{\mathrm{d}\kappa}{\mathrm{d}t} &= -\frac{1}{L}\left(R_\circ\kappa - \mathcal{E}_\circ + \frac{1}{C_\circ}\lambda\right), \\ \text{and} \quad \frac{\mathrm{d}\lambda}{\mathrm{d}t} &= \kappa. \end{aligned} \tag{2.41}$$

Physically, inductance allows specification of current, independently from charge, whereas capacitance allows specification of charge, independently from current. Thus, both quantities can be set by the user. Circuit resistance can be made zero in this case, with no further loss of generality, to obtain an LC circuit.

RL Case

Eliminating capacitors can be thought of as the circuit capacitance made infinite. The circuit equation degenerates to first order, in current:

$$\frac{\mathrm{d}\kappa}{\mathrm{d}t} = -\frac{1}{L}\left(R_\circ\kappa - \mathcal{E}_\circ\right). \tag{2.42}$$

In the context of our circuit analysis, charge is not well defined in the absence of capacitors. Thus, the user can only set current. Circuit resistance can be reduced to zero in this case too, without further alteration, to obtain an L-only circuit.

RC Case

Physically, the inductance of the proposed circuit is never exactly zero. However, we allow zero inductance in the simulation, as an approximation.

The circuit equation degenerates to first order, in charge. We thuis have

$$\frac{\mathrm{d}\lambda}{\mathrm{d}t} = \kappa = \frac{1}{R_\circ}\left(\mathcal{E}_\circ - \frac{1}{C_\circ}\lambda\right), \tag{2.43}$$

$$\text{and} \quad \frac{\mathrm{d}\kappa}{\mathrm{d}t} = \frac{1}{R_\circ}\left(\frac{\mathrm{d}\mathcal{E}_\circ}{\mathrm{d}t} - \frac{1}{C_\circ}\kappa\right). \tag{2.44}$$

In the abscence of inductance, current cannot be set independently from charge, as seen above. Charge, being the physically adjustable quantity, is the one we allow the user to set. The user is not allowed to set current directly.

In this situation, circuit resistance cannot be set to zero to obtain a C-only circuit, unless the capacitive charge exactly counters circuit emf by having $\lambda = C_\circ\mathcal{E}_\circ$. The current and the current derivative therefore become:

$$\kappa = C_\circ\frac{\mathrm{d}\mathcal{E}_\circ}{\mathrm{d}t}. \tag{2.45}$$

$$\frac{\mathrm{d}\kappa}{\mathrm{d}t} = C_\circ\frac{\mathrm{d}^2\mathcal{E}_\circ}{\mathrm{d}t^2}. \tag{2.46}$$

Due to the direct dependence on circuit emf, both charge and current cannot be set by the user in the C-only case, and no integration is carried out.

R-Only Case

Finally, with resistance alone, the differential equation degenerates to an algebraic one, which does not need integration:

$$\kappa = \frac{\mathcal{E}_\circ}{R_\circ}. \tag{2.47}$$

Here again, charge is not well defined. Furthermore, current cannot be set independently from emf and resistance. Thus, the user can set neither charge nor current. By differentiation, the derivative of the current can be evaluated as

$$\frac{\mathrm{d}\kappa}{\mathrm{d}t} = \frac{1}{R_\circ}\frac{\mathrm{d}\mathcal{E}_\circ}{\mathrm{d}t}. \tag{2.48}$$

Chapter 3

Electromagnetic Fields

In this chapter we study the electric and magnetic fields associated with the idealized circuit described in Chap. 2. We derive analytical expressions for the fields, and present the numerical procedure used to implement them.

In Sec. 3.1 we study the magnetic field, and show that its analytical expression is straightforward to evaluate. In Sec. 3.2, we identify and solve for the divergence-free and curl-free components of the electric field. We write the divergence-free component as a direct function of the magnetic field, and evaluate it accordingly. We treat the curl-free component as an electrostatic problem, derive the associated potential, and describe its numerical solution algorithmically. The analysis throughout this chapter is consistent with the assumptions of Sec. 2.3, which place us in the magnetoquasistatic approximation.

3.1 The Magnetic Field

The main simplifying assumption here is that we neglect the displacement current (Sec. 2.3). We can then write the differential Ampere-Maxwell law simply as $\nabla \times \mathbf{B} = \mu \mathbf{J}$. However, since we have uniform current density in the cylinder, it follows that the magnetic field should have cylindrical symmetry. Moreover, the invariance of the geometry under axial translation requires the magnetic field to be independent from the axial coordinate. Therefore, we must have $\mathbf{B} = \mathbf{B}(r) = B_r(r)\hat{\mathbf{r}} + B_\theta(r)\hat{\boldsymbol{\theta}} + B_z(r)\hat{\mathbf{z}}$.

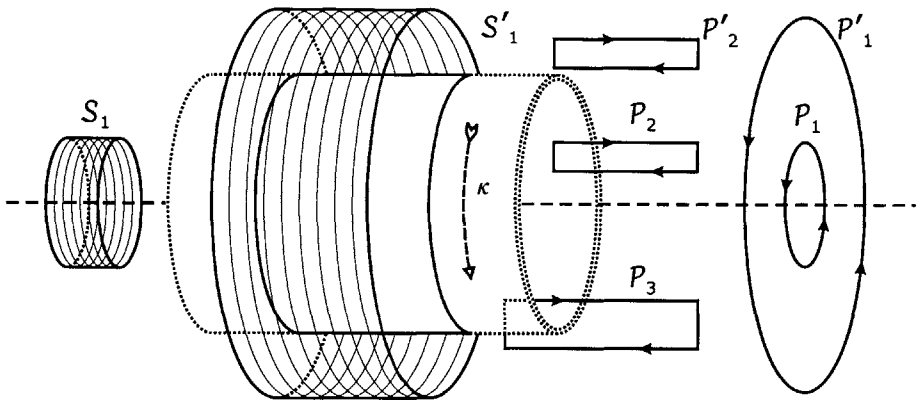

Figure 3-1: Paths and surfaces used to restrict the magnetic field expression.

We now further restrict the field expression by referring to the paths and surfaces illustrated in Fig. 3-1. Since no current flows through loops $\mathcal{P}_1$ or $\mathcal{P}'_1$, applying the integral Ampere-Maxwell law to $\mathcal{P}_1$ gives $\oint_{\mathcal{P}_1} \mathbf{B} \cdot \mathrm{dl} = \oint B_\theta(r_0) r_0 \mathrm{d}\theta = \mu I = 0$. The same thing follows for $\mathcal{P}'_1$, and therefore $B_\theta(r) = 0$, $\forall r$.

Next, we consider the outward magnetic flux for the closed surfaces $\mathcal{S}_1$ and $\mathcal{S}'_1$. The flux out of the left and right discs exactly counter each other since, taking $\hat{\mathbf{z}}$ to be to the right, $\int_{\text{left}} \mathbf{B} \cdot \mathrm{ds} = -\int_0^{2\pi} \int_0^{r_0} B_z(r) r \mathrm{d}r\mathrm{d}\theta = -\int_{\text{right}} \mathbf{B} \cdot \mathrm{ds}$. Since there are no isolated magnetic charges, the closed surface integral is zero, $\int_{\mathcal{S}_1} \mathbf{B} \cdot \mathrm{ds} = \int_{\text{left}} \mathbf{B} \cdot \mathrm{ds} + \int_{\text{right}} \mathbf{B} \cdot \mathrm{ds} + \int_{\text{cylinder}} \mathbf{B} \cdot \mathrm{ds} = 0$. This gives $\int_{\text{cylinder}} \mathbf{B} \cdot \mathrm{ds} = \int_0^{z_0} \int_0^{2\pi} B_r(r_0) r_0 \mathrm{d}\theta \mathrm{d}z = 0$ and thus $B_r(r) = 0$, $\forall r$. Therefore, we have $\mathbf{B} = B_z(r)\hat{\mathbf{z}}$.

We now consider the path integral along loops $\mathcal{P}_2$ and $\mathcal{P}'_2$. Due to the axial orientation of the field, the contribution is due entirely to the upper and lower strips. However, since no current flows through the loop, we have $\oint_{\mathcal{P}_2} \mathbf{B} \cdot \mathrm{dl} = \int_{\text{upper}} B_z(r) dz - \int_{\text{lower}} B_z(r') dz = \Delta_z(B_z(r) - B_z(r')) = 0$, and thus $B_z(r) = B_z(r') = B_{\text{in}}$ $\forall r, r' < a$ where a, as we recall, is the radus of the cylinder. Similarly, we have that $B_z(r) = B_z(r') = B_{\text{out}}$ $\forall r, r' > a$. Thus $\mathbf{B} = (B_{\text{in}} \mathscr{I}_{r<0} + B_{\text{out}} \mathscr{I}_{r>0})\hat{\mathbf{z}}$, where once again $\mathscr{I}$ is an indicator function.

For loop $\mathcal{P}_3$, there is a current $I = \Delta'_z \kappa$ flowing through, and therefore, using $\oint_{\mathcal{P}_3} \mathbf{B} \cdot \mathrm{dl} = \mu I$, we obtain

$$B_{\text{in}} - B_{\text{out}} = \mu\kappa. \tag{3.1}$$

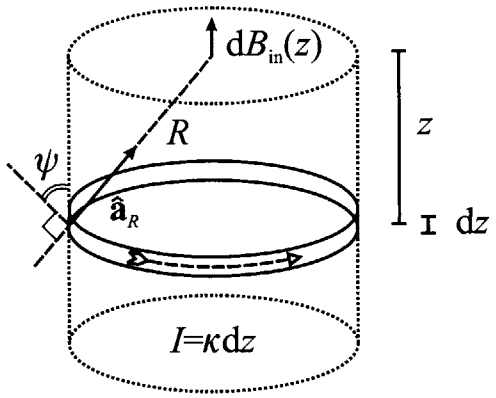

Figure 3-2: A differential strip contributes a differential amount to the inner magnetic field, which is thus the integral of all such contributions.

To obtain B_{in}, we first find the contribution $\mathrm{d}B_{\text{in}}(z)$ of a differential strip of width $\mathrm{d}z$ and centered a distance z down the axis. The current in each such strip is $I = \kappa \mathrm{d}z$. We define R to be the distance from the evaluation point to the strip, $\hat{\mathbf{a}}_R$ to be the unit vector pointing from the strip to the evaluation point, and ψ to be the angle between the axial direction and $\hat{\boldsymbol{\theta}} \times \hat{\mathbf{a}}_R$. The configuration is illustrated in Fig. 3-2. We now invoke the Biot-Savart law. We restrict ourselves to the axial component, which we know is the only survivor. Using $\mathrm{d}\mathbf{l} = a\mathrm{d}\theta\hat{\boldsymbol{\theta}}$, we write

$$\begin{aligned} \mathrm{d}B_{\text{in}}(z) &= \frac{\mu I}{4\pi}\hat{\mathbf{z}} \cdot \oint \frac{\mathrm{d}\mathbf{l} \times \hat{\mathbf{a}}_R}{R^2} = \frac{\mu I}{4\pi}\cos\psi \int_0^{2\pi} \frac{a\mathrm{d}\theta}{R^2} \\ &= \frac{\mu I a^2}{2R^3} = \frac{\mu a^2}{2(a^2+z^2)^{\frac{3}{2}}}\kappa \mathrm{d}z. \end{aligned} \tag{3.2}$$

By integrating these contributions, we obtain

$$\begin{aligned} B_{\text{in}} &= 2\int_{z=0}^{z=\infty} dB_{\text{in}}(z) = \mu\kappa \int_0^{\infty} \frac{a^2}{(a^2+z^2)^{\frac{3}{2}}}\mathrm{d}z = \mu\kappa \left.\frac{z}{(a^2+z^2)^{\frac{1}{2}}}\right|_0^{\infty} \\ &= \mu\kappa \end{aligned} \tag{3.3}$$

Eq. (3.3), together with Eq. (3.1), implies that

$$B_{\text{out}} = 0. \tag{3.4}$$

Therefore, we can write a simple expression for the magnetic field:

$$\mathbf{B} = B\hat{\mathbf{z}} = \mu\kappa\hat{\mathbf{z}}. \tag{3.5}$$

Finally, we now can give an expression for the circuit inductance L, as defined in Eq. (2.26)

$$L = \frac{\Phi}{\kappa} = \frac{\pi a^2 \mu\kappa}{\kappa} = \mu\pi a^2. \tag{3.6}$$

3.2 The Electric Field

We can decompose any vector field, and in particular the electric field $\mathbf{E}$, into a curl-free component $\mathbf{E}_\odot$ (divergence-only, irrotational) and a divergence-free component $\mathbf{E}_\otimes$ (curl-only, solenoidal). By definition: $\nabla \times \mathbf{E}_\odot = 0$, $\nabla \cdot \mathbf{E}_\otimes = 0$ and $\mathbf{E} = \mathbf{E}_\odot + \mathbf{E}_\otimes$. Such a decomposition is unique only up to *gauge transformations* [5], [10].

It then follows from Maxwell's electric field equations that $\nabla \cdot \mathbf{E}_\odot = \rho/\epsilon$ and $\nabla \times \mathbf{E}_\otimes = -\partial\mathbf{B}/\partial t$. We first obtain an explicit expression for the latter.

3.2.1 The Divergence-Free Component

By the usual symmetry argument, $\mathbf{E}_\otimes$ is invariant under axial translation. Since its source is $\mathbf{B}$, $\mathbf{E}_\otimes$ must also be cylindrically symmetric. Thus, so far, $\mathbf{E}_\otimes = E_{\otimes r}(r)\hat{\mathbf{r}} + E_{\otimes\theta}(r)\hat{\boldsymbol{\theta}} + E_{\otimes z}(r)\hat{\mathbf{z}}$.

Next, we invoke Stoke's theorem to loop $\mathcal{P}_1$ in Fig. 3-1:

$$\begin{aligned} \oint_{\mathcal{P}_1} \mathbf{E}_\otimes \cdot \mathrm{ds} &= -\iint \frac{\partial \mathbf{B}}{\partial t} = -\pi r_0^2 \mu \frac{\mathrm{d}\kappa}{\mathrm{d}t} \\ &= 2\pi r_0 E_{\otimes\theta}(r_0) \end{aligned} \tag{3.7}$$

A similar invokation For the outer loop $\mathcal{P}_1'$ gives:

$$\begin{aligned} \oint_{\mathcal{P}_1'} \mathbf{E}_\otimes \cdot \mathrm{ds} &= -\iint \frac{\partial \mathbf{B}}{\partial t} = -\pi a^2 \mu \frac{\mathrm{d}\kappa}{\mathrm{d}t} \\ &= 2\pi r_0' E_{\otimes\theta}\theta(r_0') \end{aligned} \tag{3.8}$$

These two equations determine the angular component everywhere. However, we now go a step further and claim that the curl-only field is well defined with this component alone, i.e.

$$\mathbf{E}_{\otimes} = \left\{ \begin{array}{ll} -r/2 & \text{for } r < a \\ -a^2/2r & \text{for } r > a \end{array} \right\} \mu \frac{\mathrm{d}\kappa}{\mathrm{d}t} \hat{\boldsymbol{\theta}} \tag{3.9}$$

Indeed, based on Eq. (3.5), we have that $\nabla \times \mathbf{E}_{\otimes} = \frac{1}{r}\frac{\partial}{\partial r}(rE_{\otimes})\hat{\mathbf{z}} = -\frac{\partial \mathbf{B}}{\partial t}$, verifying this Maxwell's equation. Moreover, $\nabla \cdot \mathbf{E}_{\otimes} = \frac{1}{r}\frac{\partial}{\partial \theta}(E_{\otimes}) = 0$, thus $\mathbf{E}_{\otimes}$ is indeed divergence-free, as we expect.

As a consequence of the fact that $\nabla \cdot \mathbf{B} = 0$, the total electric field can always be written, again up to gauge transformations, as a function of the magnetic vector potential $\mathbf{A}$, defined by $\mathbf{B} = \nabla \times \mathbf{A}$, and a scalar potential V, as follows:

$$\mathbf{E} = -\nabla V - \frac{\partial \mathbf{A}}{\partial t}. \tag{3.10}$$

We can now make the identification $\mathbf{E}_{\otimes} = -\frac{\partial \mathbf{A}}{\partial t}$, by the following choice of magnetic vector potential:

$$\mathbf{A} = \left\{ \begin{array}{ll} -r/2 & \text{for } r < a \\ -a^2/2r & \text{for } r > a \end{array} \right\} \mu\kappa\hat{\boldsymbol{\theta}}. \tag{3.11}$$

3.2.2 The Curl-Free Component

We now consider $\mathbf{E}_{\odot}$. The choice of magnetic vector potential, Eq. (3.11) above, simplifies our analysis considerably. In fact, the problem is reduced to an equivalent electrostatic one, since

$$\mathbf{E}_{\odot} = \mathbf{E} - \mathbf{E}_{\otimes} = -\nabla V. \tag{3.12}$$

Just as in electrostatics, $\mathbf{E}_{\odot}$ is completely determined once the scalar potential is defined everywhere in space. Furthermore, we have $\nabla \cdot \mathbf{A} = 0$. As a result, V satisfies Poisson's equation, and the electrostatic analogy is made complete:

$$\nabla^2 V = \nabla \cdot E - \frac{\partial}{\partial t}(\nabla \cdot \mathbf{A}) = \nabla \cdot E = -\rho/\epsilon. \tag{3.13}$$

Again, the problem is invariant under axial translation, which implies that the scalar potential is independent of the axial component, z. Hence, we denote it by $V(r, \theta)$.

General Solution for the Potential

As there are no charges anywhere except for the surface of the cylinder, Poisson's equation reduces to Laplace's equation, and $V(r, \theta)$, $\forall r \neq a$, is a solution of $\nabla^2 V = 0$. Since this is a linear equation, the general solution will be a linear combination of all possible special solutions. To find the special solutions, we apply the separation $V_1(r)V_2(\theta)$, to write the Laplacian as follows:

$$\nabla^2 V = \frac{1}{r}\frac{\partial}{\partial r}\left(r\frac{\partial V_1}{\partial r}\right)V_2 + \frac{1}{r^2}\frac{\partial^2 V_2}{\partial \theta^2}V_1. \tag{3.14}$$

Setting this to zero, we obtain:

$$-\frac{1}{V_2}\frac{\partial^2 V_2}{\partial \theta^2} = \frac{r}{V_1}\frac{\partial}{\partial r}\left(r\frac{\partial V_1}{\partial r}\right) = K. \tag{3.15}$$

The first equation embedded in Eq. (3.15) is

$$\frac{\partial^2 V_2}{\partial \theta^2} + KV_2 = 0. \tag{3.16}$$

Solutions to Eq. (3.16) must be of the form $e^{j\sqrt{K}\theta}$. Several restrictions will shape the solution space. First, V_2 must be single valued, and thus the solution needs to be periodic, of period 2π. This means that $\sqrt{K}$ must be a real integer: $\sqrt{K} = n$, where $n \in \mathbb{Z}$. Second, solutions defined as such will be complex, thus only real linear combinations for the general solution will eventually be admitted. This will be satisfied by imposing the boundary condition on the surface of the cylinder.

The second equation in Eq. (3.15) is

$$r^2\frac{\partial^2 V_1}{\partial r^2} + r\frac{\partial V_1}{\partial r} - n^2 V_1 = 0. \tag{3.17}$$

The solutions to Eq. (3.17) must be of the form r^m. By substituting this form in the equation, we see that $m = \pm n$. This links the solutions for V_1 and V_2 to yield $r^m e^{jn\theta}$ as all possible special solutions to Laplace's equation. Thus, using linearity, the general solution is

$$V(r,\theta) = \sum_{n=-\infty}^{\infty} A_n r^m e^{jn\theta}. \tag{3.18}$$

Surface Potential

Before proceeding, we express the scalar potential on the surface of the cylindrical shell in terms of the circuit quantities developed in Chap. 2. For the sake of notation, we drop the r dependence, and denote this *surface potential* by $V(\theta) = V(a,\theta)$.

Scalar potentials that differ by a constant are equivalent in terms of the field they represent. Therefore, we start by specifying a "ground" angle to be our reference point. We choose $V(0) = 0$, for convenience. In these terms, we have (without bothering to introduce an auxiliary integration variable):

$$\begin{aligned} V(\theta) &= \int \mathbf{E}_{\odot} \cdot \mathrm{dl} \\ &= \int_0^{\theta} \mathbf{E}_{\odot} \cdot \hat{\boldsymbol{\theta}} a \mathrm{d}\theta. \end{aligned} \tag{3.19}$$

We recall the expression of the total electric field from Eq. (2.29) to be

$$\mathbf{E} = \left[\rho_{\delta}(\theta)\kappa - f(\theta) + \sum_i \mathscr{I}_i(\theta) \frac{\lambda}{\epsilon \ell_i} \right] \hat{\boldsymbol{\theta}}.$$

However, we have that $\mathbf{E}_{\odot} = \mathbf{E} - \mathbf{E}_{\otimes}$, and we know from Eq. (3.9) that the curl-free component evaluates to $-\mu \frac{a}{2} \frac{\mathrm{d}\kappa}{\mathrm{d}t} \hat{\boldsymbol{\theta}}$ on the surface.

Thus,

$$\begin{aligned} V(\theta) &= \int_0^{\theta} \mathbf{E} \cdot \hat{\boldsymbol{\theta}} a \mathrm{d}\theta - \int_0^{\theta} \mu \frac{a^2}{2} \frac{\mathrm{d}\kappa}{\mathrm{d}t} \mathrm{d}\theta \\ &= \int_0^{\theta} \left[\rho_{\delta}(\theta)\kappa - f(\theta) + \sum_i \mathscr{I}_i(\theta) \frac{\lambda}{\epsilon \ell_i} \right] a \mathrm{d}\theta - \mu \frac{a^2}{2} \frac{\mathrm{d}\kappa}{\mathrm{d}t} \theta. \end{aligned} \tag{3.20}$$

The last term in the above expression is of special interest. Using Eq. (3.6), i.e. $L = \mu\pi a^2$, we see that its total contribution to the scalar potential is $-L\frac{\mathrm{d}\kappa}{\mathrm{d}t}$. This is nothing but familiar *induced emf*, associated with the circuit inductance. Its pointwise contribution is a steady ramp, whose effect is to remove the discontinuity that would have otherwise resulted had we just treated the problem as an electrostatic one, and integrated the total electric field $\mathbf{E}$.

As we have seen in Sec. 2.4.2, we typically want to work with discrete components (resistors, batteries and capacitors), which correspond to sections with uniform properties. Recall that within the extent of each component $\mathcal{C}$ in this discrete component model the electric field is a constant of the form $\mathbf{E}_{\mathcal{C}} = E_{\mathcal{C}}\hat{\boldsymbol{\theta}}$. From this fact and Eq. (3.20), we see that each such component would contribute to the total scalar potential a ramp-step function $V_{\mathcal{C}}(\theta)$ of slope $aE_{\mathcal{C}}$. Considering the circuit inductance a component as well, as it contributes a similar ramp, we will have $V(\theta) = \sum_{\mathcal{C}} V_{\mathcal{C}}(\theta)$. For example, a resistor R_i with extent $\Delta\theta_{R_i}$ and starting angle $\theta^\star_{R_i}$ has $E_{R_i} = \kappa R_i/(a\Delta\theta_{R_i})$ by Eq. (2.38), and thus its contribution is:

$$V_{R_i}(\theta) = \begin{cases} 0 & 0 \le \theta < \theta^\star_{R_i} \\ \kappa R_i(\theta - \theta^\star_{R_i})/\Delta\theta_{R_i} & \theta^\star_{R_i} \le \theta \le \theta^\star_{R_i} + \Delta\theta_{R_i} \\ \kappa R_i & \theta^\star_{R_i} + \Delta\theta_{R_i} < \theta < 2\pi \end{cases} . \tag{3.21}$$

For batteries and for capacitors we use Eq. (2.39) and Eq. (2.40) respectively to obtain similar expressions. Combining these with the ramp due to circuit inductance, we now have a practical scheme to evaluate $V(\theta)$ numerically:

$$\begin{aligned} V(\theta) = \quad & \sum_i \kappa R_i \Big\langle \frac{(\theta - \theta^\star_{R_i})}{\Delta\theta_{R_i}} \Big\rangle \\ & - \sum_i \mathcal{E}_i \Big\langle \frac{(\theta - \theta^\star_{\mathcal{E}_i})}{\Delta\theta_{\mathcal{E}_i}} \Big\rangle \\ & + \sum_i \frac{\lambda}{C_i} \Big\langle \frac{(\theta - \theta^\star_{C_i})}{\Delta\theta_{C_i}} \Big\rangle - L\frac{\mathrm{d}\kappa}{\mathrm{d}t}\frac{\theta}{2\pi}, \end{aligned} \qquad \text{where } \langle x \rangle \triangleq \begin{cases} 0 & x < 0 \\ x & 0 \le x \le 1 \\ 1 & x > 1 \end{cases} . \tag{3.22}$$

Boundary Condition

The surface scalar potential is now specified as a continuous function $V(\theta)$ of the θ coordinate. Naturally, it is single valued and is thus periodic, of period 2π, and can be Fourier-expanded as follows:

$$V(\theta) = V(r,\theta)|_{r=a} = \sum_{n=-\infty}^{\infty} C[n]e^{jn\theta}, \tag{3.23}$$

where $C[n]$ is the Fourier series of $V(\theta)$, given by

$$C[n] = \frac{1}{2\pi}\int_0^{2\pi} V(\theta)e^{-jn\theta}\mathrm{d}\theta. \tag{3.24}$$

Eq. (3.23) is a convenient form for the boundary condition imposed on Eq. (3.18), since by direct comparison we obtain the condition $A_n a^m = C[n]$, and thus $A_n = \frac{1}{a^m}C[n]$. This allows us to write:

$$V(r,\theta) = \sum_{n=-\infty}^{\infty} \left(\frac{r}{a}\right)^m C[n]e^{jn\theta}. \tag{3.25}$$

The final detail to settle is to determine m, as it can be n or $-n$. Since we require the potential to be well behaved, it is necessary for the power term to die out. This dictates the following conditions: if $(r < a)$ and $(n > 0)$ then $m = n$, if $(r < a)$ and $(n < 0)$ then $m = -n$, if $(r > a)$ and $(n > 0)$ then $m = -n$, and if $(r > a)$ and $(n < 0)$ then $m = n$.

We can summarize these conditions in the following compact expression:

$$V(r,\theta) = \sum_{n=-\infty}^{\infty} \underbrace{\left(\frac{r}{a}\right)^{s|n|} C[n]}_{C_V[n]} e^{jn\theta}. \tag{3.26}$$

Here $s = \text{sgn}(a - r)$, where sgn(.) stands for the *signum* function,

$$\text{sgn}(x) \triangleq \begin{cases} -1 & x < 0 \\ 0 & x = 0 \\ +1 & x > 0 \end{cases}.$$

Thus, s is $+1$ inside the cylinder, and -1 outside of it. By convention, s is zero for a zero argument, i.e. on the surface of the cylinder. This is of no consequence, since when $r = a$, we have a unity exponentiation.

Electric Field and Surface Charge Density

To obtain the electric field we write the gradient equation in cylindrical coordinates: $\mathbf{E}_{\odot} = E_{\odot r}\hat{\mathbf{r}} + E_{\odot\theta}\hat{\boldsymbol{\theta}} + E_{\odot z}\hat{\mathbf{z}} = -\nabla V$,

$$\begin{aligned} E_{\odot r} &= -\frac{\partial V}{\partial r} \\ &= \sum_{n=-\infty}^{\infty} \left(-\frac{\partial}{\partial r} C_V[n]\right) e^{jn\theta} \\ &= \sum_{n=-\infty}^{\infty} \underbrace{-\frac{s|n|}{r}\left(\frac{r}{a}\right)^{s|n|} C[n]}_{C_{E_{\odot r}}[n]} e^{jn\theta}, \end{aligned} \tag{3.27}$$

$$\begin{aligned} E_{\odot\theta} &= -\frac{1}{r}\frac{\partial V}{\partial \theta} \\ &= \sum_{n=-\infty}^{\infty} -\frac{1}{r} C_V[n] \left(\frac{\partial}{\partial \theta} e^{jn\theta}\right) \\ &= \sum_{n=-\infty}^{\infty} \underbrace{\left(\frac{-jn}{r}\left(\frac{r}{a}\right)^{s|n|}\right) C[n]}_{C_{E_{\odot\theta}}[n]} e^{jn\theta}, \end{aligned} \tag{3.28}$$

and

$$E_{\odot z} = \frac{\partial V}{\partial z} = 0. \tag{3.29}$$

Finally, the surface charge density can be obtained by applying Gauss's law on a thin Gaussian angular box surrounding a portion of the shell, and of cylindrical dimensions $(\Delta r, \Delta\theta, \Delta z)$, where Δr is negligible compared to the other dimensions. The area of the face of the box along the shell is $\Delta S = a\Delta\theta\Delta z$. At the limit when $\Delta\theta \to 0$:

$$\iint \mathbf{E} \cdot d\mathbf{s} = \mathbf{E}|_{r=R^+} \cdot (\Delta S\hat{r}) + \mathbf{E}|_{r=R^-} \cdot (-\Delta S\hat{r}) = \sigma(\theta)\Delta S/\epsilon, \tag{3.30}$$

from which we obtain

$$\begin{aligned} \sigma(\theta) &= \epsilon\left(E_{\odot r}|_{r=R^+} - E_{\odot r}|_{r=R^-}\right) \\ &= \sum_{n=-\infty}^{\infty} \underbrace{\epsilon\left(\frac{2|n|}{a}\right) C[n]}_{C_\sigma[n]} e^{jn\theta}. \end{aligned} \tag{3.31}$$

3.2.3 Numerical Computation

One of the obstacles in the numerical computation of the analytical solutions is the fact that the surface scalar potential $V(\theta)$ is defined as a continuous function. This, for instance, entails the numerical evaluation of a continuous integral, as given by Eq. (3.24). In the subsequent sections we show how it is possible to define and operate on only discrete quantities from the beginning. The approach parallels well-known techniques in discrete-time signal processing.

Discretization of the Surface Potential

Let us assume that the surface potential is such that the Fourier series coefficients satisfy the following condition:

$$\forall\epsilon > 0 \quad \exists N : |C[n]| < \epsilon, \forall n \notin \left[\lceil\frac{N}{2}\rceil - N, \lceil\frac{N}{2}\rceil - 1\right], \tag{3.32}$$

in other words, we assume they are effectively zero beyond a block of length N around 0, with the centering perfect or not, based on whether N is odd or even.

This is a reasonable requirement, which will be violated only if there are sharp discontinuities, such as Dirac delta functions or steps, in $V(\theta)$. This finite length property allows us to extend $C[n]$ by introducing periodic images of itself every N samples, as follows:

$$\tilde{C}[n] = \sum_{m=-\infty}^{\infty} C[n - mN]. \tag{3.33}$$

Since no non-zero coefficients overlap, we can extract the original coefficients perfectly from this periodic extension. Specifically, indices $n \in [0, N-1]$ contain all the original non-zero coefficients in the following fashion: $\tilde{C}[n] = C[n]$ for $n \in \left[0, \lceil \frac{N}{2} \rceil - 1\right]$, and $\tilde{C}[n] = C[n-N]$ for $n \in \left[\lceil \frac{N}{2} \rceil, N-1\right]$.

The reason we introduced $\tilde{C}[n]$ is that it admits a *discrete* inverse[1] Fourier series expansion. The discreteness of this inverse Fourier series is due to the periodicity of $\tilde{C}[n]$, in contrast to $C[n]$, which has a *continuous* inverse Fourier transform, $V(\theta)$. The forward and inverse discrete Fourier series equations, respectively, are:

$$\tilde{C}[n] = \frac{1}{N} \sum_{k=0}^{N-1} V[k] e^{-j2\pi nk/N}, \tag{3.34}$$

and

$$V[k] = \sum_{n=0}^{N-1} \tilde{C}[n] e^{j2\pi nk/N}. \tag{3.35}$$

As can be seen, $V[k]$ is itself periodic, of period N, and only the Ndistinct samples are needed to reconstruct $\tilde{C}[n]$ in Eq. (3.34). As our notation suggests, our new goal is to relate $V[k]$ to $V(\theta)$, which we will do in a series of manipulations. First, let us split the summation in a way such that we can use the extraction scheme we mentioned above, to replace $\tilde{C}[n]$ by $C[n]$ in the first part, and by $C[n-N]$ in the second:

$$V[k] = \sum_{n=0}^{\lceil \frac{N}{2} \rceil - 1} C[n] e^{j2\pi nk/N} + \sum_{n=\lceil \frac{N}{2} \rceil}^{N-1} C[n-N] e^{j2\pi nk/N}. \tag{3.36}$$

[1]We have used the term "inverse" to indicate the negative signs in the harmonics, i.e. here we are thinking of $\frac{1}{N}V[k]$ as a harmonic expansion of $\tilde{C}[n]$, but there is a negative sign in all the exponentials in Eq. (3.34).

Now, let's define $l = n - N$, and proceed to remerge the two summations:

$$\begin{aligned} V[k] &= \sum_{n=0}^{\lceil \frac{N}{2} \rceil - 1} C[n] e^{j2\pi nk/N} + \sum_{l=\lceil \frac{N}{2} \rceil - N}^{-1} C[l] \underbrace{e^{j2\pi(l+N)k/N}}_{e^{j2\pi lk/N}} \\ &= \sum_{n=\lceil \frac{N}{2} \rceil - N}^{\lceil \frac{N}{2} \rceil - 1} C[n] e^{j2\pi nk/N} \\ &= \sum_{n=-\infty}^{\infty} C[n] e^{j2\pi nk/N} \end{aligned} \tag{3.37}$$

In the last equality, we have used the fact that $C[n]$ is effectively zero beyond $n \in \left[\lceil \frac{N}{2} \rceil - N, \lceil \frac{N}{2} \rceil - 1\right]$, to extend the summation to $[-\infty, \infty]$, by including the zero coefficients. The final manipulation is to replace $C[n]$ with its expression in terms of $V(\theta)$ as given by Eq. (3.24), to obtain:

$$\begin{aligned} V[k] &= \sum_{n=-\infty}^{\infty} \left[\frac{1}{2\pi} \int_0^{2\pi} V(\theta) e^{-jn\theta} \mathrm{d}\theta \right] e^{j2\pi nk/N} \\ &= \frac{1}{2\pi} \int_0^{2\pi} V(\theta) \underbrace{\left[\sum_{n=-\infty}^{\infty} e^{-jn(\theta - 2\pi k/N)} \right]}_{\sum_{m=-\infty}^{\infty} 2\pi\delta(\theta - 2\pi k/N - 2\pi m)} \mathrm{d}\theta \\ &= V(2\pi k/N). \end{aligned} \tag{3.38}$$

For the last substitution, we have used the fact that $\sum_{n=-\infty}^{\infty} e^{-jn(\theta - 2\pi k/N)}$ is the expression for the discrete-time Fourier transform of $e^{j2\pi nk/N}$, which can be shown to be the periodic impulse train $\sum_{m=-\infty}^{\infty} 2\pi\delta(\theta - 2\pi k/N - 2\pi m)$, of period 2π. Of these impulses, only one lies in the $[0, 2\pi]$ integration interval, the one at $\theta = 2\pi k/N$, which sifts out $V(2\pi k/N)$.

From Eq. (3.38), we can see that $V[k]$ is a discretized, i.e. sampled, version of the continuous $V(\theta)$, with N samples taken starting from $\theta = 0$, at sampling intervals of $2\pi/N$.

Discretization of Derived Quantities

The discretization thus far allows us to define the surface potential by N of its samples. From these, $\tilde{C}[n]$ can be computed using the discrete summation in Eq. (3.34). Then, $C[n]$ is immediately obtained by extraction, thus avoiding continuous integration as required by Eq. (3.24). Once $C[n]$ is known, all the derived quantities, i.e. the potential everywhere, the electric field components, and the surface charge density can be computed, since they all can be written in the following general form [cf. equations Eq. (3.26), Eq. (3.27), Eq. (3.28), and Eq. (3.31)]:

$$F = \sum_{n=-\infty}^{\infty} C_F[n] e^{jn\theta} = \sum_{n=-\infty}^{\infty} \alpha_F[n] C[n] e^{jn\theta}. \tag{3.39}$$

We now would like to express these quantities in the discrete context, by writing them in terms of $\tilde{C}[n]$ directly. This allows us to completely avoid using $C[n]$, which in turn streamlines the computation. For this, we assume that $C_F[n]$ satisfies the property established in Eq. (3.32), despite the multiplicative factor of $\alpha_F[n]$. Thus, we can proceed in the reverse order as we did before:

$$\begin{aligned}
F &= \sum_{n=-\lceil \frac{N}{2} \rceil - N}^{\lceil \frac{N}{2} \rceil - 1} \alpha_F[n] C[n] e^{jn\theta} \\
&= \sum_{n=0}^{\lceil \frac{N}{2} \rceil - 1} \alpha_F[n] C[n] e^{jn\theta} + \sum_{n=\lceil \frac{N}{2} \rceil - N}^{-1} \alpha_F[n] C[n] e^{jn\theta} \\
&= \sum_{n=0}^{\lceil \frac{N}{2} \rceil - 1} \alpha_F[n] \tilde{C}[n] e^{jn\theta} + \sum_{l=\lceil \frac{N}{2} \rceil}^{N-1} \alpha_F[l-N] C[l-N] e^{j(l-N)\theta} \\
&= \sum_{n=0}^{\lceil \frac{N}{2} \rceil - 1} \tilde{\alpha}_F[n] \tilde{C}[n] e^{jn\theta} + \sum_{l=\lceil \frac{N}{2} \rceil}^{N-1} \tilde{\alpha}_F[l] \tilde{C}[l] e^{j(l-N)\theta}.
\end{aligned} \tag{3.40}$$

In Eq. (3.40), $\tilde{\alpha}_F[n]$ is the periodic extension of $\alpha_F[n]$, after it is limited to $n \in \left[\lceil \frac{N}{2} \rceil - N, \lceil \frac{N}{2} \rceil - 1\right]$:

$$\tilde{\alpha}_F[n] = \begin{cases} \alpha_F[n] & ;\ n \in \left[0, \lceil \frac{N}{2} \rceil - 1\right] \\ \alpha_F[n-N] & ;\ n \in \left[\lceil \frac{N}{2} \rceil, N-1\right] \\ \tilde{\alpha}_F[n-mN] & ;\ \forall (n,m) \in \mathbb{Z}^2 \end{cases} . \tag{3.41}$$

At this point, it is desirable to merge the two summations in Eq. (3.40) into one that extends over $n \in [0, N]$. That requires eliminating the $e^{-jN\theta}$ factor in the second summation, which can be done only if θ is an integer multiple of $2\pi/N$. However, we can always express an arbitrary angle as $\theta = 2\pi m/N + \phi$, where $m \in \mathbb{Z}$, and $0 \leq \phi < 2\pi/N$. With this notation, we can write:

$$\begin{aligned} F &= \sum_{n=0}^{\lceil \frac{N}{2} \rceil - 1} \tilde{\alpha}_F[n]\tilde{C}[n] \exp\Big[jn(2\pi k/N + \phi)\Big] \\ &\quad + \sum_{l=\lceil \frac{N}{2} \rceil}^{N-1} \tilde{\alpha}_F[l]\tilde{C}[l] \exp\Big[j(l-N)(2\pi k/N + \phi)\Big] \\ &= \sum_{n=0}^{\lceil \frac{N}{2} \rceil - 1} \tilde{\alpha}_F[n]\tilde{C}[n] \exp\Big(j2\pi nk/N\Big) \cdot \exp\Big[jn\phi\Big] \\ &\quad + \sum_{n=\lceil \frac{N}{2} \rceil}^{N-1} \tilde{\alpha}_F[n]\tilde{C}[n] \exp\Big(j2\pi nk/N\Big) \cdot \exp\Big[j(n-N)\phi\Big]. \end{aligned} \tag{3.42}$$

Now, when ϕ is zero, F is defined only at N samples around the circumference of radius r, as k varies from 0 to N. This allows for the introduction of a discrete version of the derived quantity, say $F[k]$, analogously to $V[k]$, the discrete surface potential. In this case, the expression becomes [cf. Eq. (3.35)]:

$$F[k] = \sum_{n=0}^{N} \underbrace{\tilde{\alpha}_F[n]\tilde{C}[n]}_{\tilde{C}_F[n]} e^{j2\pi nk/N}. \tag{3.43}$$

In this light, it is clear that the $e^{jn\phi}$ and $e^{j(n-N)\phi}$ factors in Eq. (3.42) perform an interpolation between the N samples, at a shift of ϕ from the original discrete angles. In fact, $e^{jn\phi}$ represents the discretized transfer function of a *fractional sample advance*, as referred to in the discrete-time signal processing literature.

Finally, Eq. (3.43) can be readily identified as an inverse discrete Fourier series , and we can write the forward equation [c.f. Eq. (3.34)] as:

$$\tilde{C}_F[n] = \frac{1}{N}\sum_{k=0}^{N} F[k]e^{-j2\pi nk/N}. \tag{3.44}$$

Numerical Computation

As we have see in Sec. 3.2.2, once the circuit quantities are obtained according to the description in Chap. 2, Sec. 2.4, we can evaluate $V(\theta)$ at any θ on the surface of the cylinder. With this information, the computation of all quantities, $F \in \{V, E_{\odot r}, E_{\odot\theta}, \sigma\}$, at position (r, θ), takes the following algorithmic form:

A. Discrete Surface Potential

Obtain the samples $V[k]$ by evaluating $V(2\pi k/N)$, for $k = 0, \cdots, N-1$.

B. Surface Potential Coefficients

Compute the DFT of $V[k]$ to obtain $\tilde{C}[n]$, for $n = 0, \cdots, N-1$.

C. $\tilde{\alpha}_F$ Factors

Compute the $\tilde{\alpha}_F[n]$ factors for $n = 0, \cdots, N-1$, using the r coordinate, according to the appropriate equation, Eq. (3.26), Eq. (3.27), Eq. (3.28), or Eq. (3.31), and the extension equation, Eq. (3.41).

D. Derived Coefficients

Compute the $\tilde{C}_F[n]$ coefficients as $\tilde{\alpha}_F[n]\tilde{C}[n]$, according to Eq. (3.43).

E. Derived Quantity

Evaluate the interpolated inverse DFT according to Eq. (3.42), using the θ coordinate to find ϕ, such as $\theta = 2\pi m/N + \phi$, where $m \in \mathbb{Z}$, and $0 \leq \phi < 2\pi/N$.

The discrete Fourier transform (DFT) acronym that we have used in steps **B** and **E** above, is directly related to the discrete Fourier series (DFS), given by the forward and inverse equations in Eq. (3.34) [or Eq. (3.44)] and Eq. (3.35) [or Eq. (3.43)], respectively. As we have seen, both $\tilde{C}[n]$ and $V[k]$ are periodic, of period N, and the same applies to $\tilde{C}_F[n]$ and $F[k]$, for all derived quantities. The DFT formalism extends the DFS to finite-length, and thus aperiodic, sequences. The N samples of such a sequence are treated as the distinct samples of a hypothetical periodic extension. In this sense, and since the DFS equations only operate on these N distinct samples the defining equations of the DFT are exactly the same. In fact, for the purpose of the current discussion, there is no need to introduce the DFT, since our sequences are indeed periodic. The only reason we do so is that the fast Fourier transform (FFT) algorithm is usually introduced in the DFT context, rather than that of the DFS.

Gauss was probably the first to have obtained an FFT-like algorithm [4]. However, in its modern incarnation, FFT is due to Cooley and Tukey [3]. The algorithm computes the *complete* DFT, or inverse DFT, of a sequence, i.e. all N transfrom values, in only $O(N \log N)$ arithemtic operations, by exploiting redundancies in the structure of the problem, which if done directly using Eq. (3.34) or Eq. (3.35) would require N complex multiplications and $N-1$ complex additions per transform value, for a total of $O(N^2)$ operations. It is to emphasize that when only one transform value is to be computed, we need to revert back to direct computation, consuming thus $O(N)$ operations. Clearly, the FFT applies only to step **B** above, where all values of $\tilde{C}[n]$ are computed. In step **E**, F is evaluated at a single point, and direct summation needs to be used.

Chapter 4

Energy Flow

In this chapter we proceed to study and visualize the electromagnetic energy carried by the electromagnetic fields derived in Chap. 3, and associated with the idealized electric circuit described in Chap. 2.

In Sec. 4.1, we present the notion of electromagnetic energy density and give the energy conservation equation. We interpret this as a continuous flow equation and, in Sec. 4.2, we implement this interpretation as the flow of quantized energy particles, by describing their evolution, creation and destruction. This gives us a meaningful way to visualize the flow of energy in our electric circuit.

4.1 Electromagnetic Energy

We adopt the view that electromagnetic energy is stored in the field [5], and described by the energy density

$$u(r,\theta) = \frac{\epsilon}{2}E^2 + \frac{1}{2\mu}B^2, \tag{4.1}$$

where E and B are the magnitudes of the electric and magnetic fields respectively.

Eq. (4.1) is a volume differentiated version of the total electric and magnetic energies associated with the respective fields. Electric energy is the work required to start with charges spread out at infinity and configure them, against the electric force, into a charge density that establishes the given electric field.

Magnetic energy, on the other hand, is the work required to start with no current and obtain, against back emf, a curent density that establishes the given magnetic field. From Maxwell's equation, one can directly derive the following conservation equation:

$$\frac{\partial}{\partial t}u + \nabla \cdot \boldsymbol{\mathcal{P}} = -\mathbf{J} \cdot \mathbf{E}, \tag{4.2}$$

where

$$\boldsymbol{\mathcal{P}} = \frac{1}{\mu}\mathbf{E} \times \mathbf{B} \tag{4.3}$$

is the *Poynting vector* field.

We can identify Eq. (4.2) with a flow equation

$$\frac{\partial}{\partial t}u + \nabla \cdot (u\mathbf{v}) = \varsigma \tag{4.4}$$

by defining the velocity field $\mathbf{v}$ and the source-sink field ς as follows:

$$\mathbf{v} = \frac{1}{u}\boldsymbol{\mathcal{P}} = 2\frac{\mathbf{E} \times \mathbf{B}}{\mu\epsilon E^2 + B^2}, \tag{4.5}$$

$$\text{and} \quad \varsigma = -\mathbf{J} \cdot \mathbf{E}. \tag{4.6}$$

When applied to our problem, the first observation we can make about this flow interpretation is that all energy sources and sinks are on the surface of the shell, since the current density $\mathbf{J}$ is zero everywhere else.

Next, recall from Eq. (3.4) that there is no magnetic field outside the cylinder, therefore $\mathbf{v}$ is zero there, and there is no energy flow there. How, then, does u vary there, since based on Eq. (4.1) and the variation of E, it clearly does? The answer to that lies in the magnetoquasistatic approximation from Sec. 2.3 and the fact that the displacement current, which is proportional to the time variation of the electric field, is negligible, Eq. (2.27). Therefore, to conclude, if we are to visualize energy flow, it is enough to consider only the inside of the cylinder.

4.2 Flow Visualization

4.2.1 Discretization of Energy Flow

In this section we propose a straightforward discretization of the continuous flow of electromagnetic energy of Sec. 4.1. We think of continuous flow as a discrete flow of *energy particles* carrying a fixed energy quantum ε. The simulation then has to manage a *particle system.* Assuming the distribution of these particles is consistent with the underlying energy density, it suffices to evolve them according to the velocity $\mathbf{v}$ to obtain a crude approximation to the actual flow in regions of no sources or sinks, i.e. strictly inside the cylinder.

As in Sec. 2.4.3, we assume the availability of a solver for systems of first order differential equations. Since we have already shown how to numerically obtain the electromagnetic fields in Chap. 3, and since $\mathbf{v}$ is a function of $\mathbf{E}$ and $\mathbf{B}$, the description of the evolution of energy particles is complete.

Before we proceed, note that since there are two components to the total energy density, we can visualize the energy balance between electric and magnetic fields by coloring the particle. Let $\mathbf{C}$ indicate the particle color vector. An appealing visualization is to specify a characteristic color for each field type, say $\mathbf{C_E}$ and $\mathbf{C_B}$ for the electric and magnetic colors respectively, then interpolate the particle color between these based on the energy ratio:

$$\mathbf{C} = \alpha \mathbf{C_E} + (1-\alpha)\mathbf{C_B}, \qquad \text{where } \alpha = \frac{\frac{\epsilon}{2}E^2}{\frac{\epsilon}{2}E^2 + \frac{1}{2\mu}B^2}. \tag{4.7}$$

4.2.2 Particle Destruction and Creation

We now have to deal with sinks and sources: particles should be created and destroyed appropriately on the surface of the cylinder, at a rate governed by ς. Particle destruction is easy, we simply remove particles flowing into the surface. We study particle creation more carefully. To simplify both management and computation, we consider exclusively the discrete component model of Sec. 2.4.2 and Sec. 3.2.2.

We know that each component $\mathcal{C}$, in this case, has an electric field that is constant within its extent $\mathbf{E}_{\mathcal{C}} = E_{\mathcal{C}}\hat{\boldsymbol{\theta}}$. Connective sections have zero electric field, as noted in Sec. 2.4.1. The current density being constant everywhere, this means that the rate of energy production or dissipation is uniform over the extent of the component. The total rate per unit length along the cylinder axis and over the extent of a component gives us the power per unit length associated with that component:

$$P_{\mathcal{C}} = \int_{\theta_{\mathcal{C}}^{\star}}^{\theta_{\mathcal{C}}^{\star}+\Delta\theta_{\mathcal{C}}} \int_{a-\delta/2}^{a+\delta/2} -\mathbf{J}\cdot\mathbf{E}\, r\mathrm{d}r\mathrm{d}\theta = (a\Delta\theta_{\mathcal{C}})E_{\mathcal{C}}\kappa \qquad \mathrm{W/m} \tag{4.8}$$

The power expressions for each type of component can be obtained using Eq. (2.38), Eq. (2.39) and Eq. (2.40):

$$P_{R_i} = R_i\kappa^2, \tag{4.9}$$

$$P_{\mathcal{E}_i} = -\mathcal{E}_i\kappa, \tag{4.10}$$

$$P_{C_i} = \frac{\lambda}{C_i}\kappa. \tag{4.11}$$

By integrating power, using the differential equation solver, we obtain the instantaneous amount of energy $W_{\mathcal{C}}$ produced or dissipated by any given component.

In this discrete flow setting, it is reasonable to create particles in batches. For a batch size of N_ε this scheme consists of waiting until the increment of $W_{\mathcal{C}}$ reaches $\varepsilon N_\varepsilon$ as compared to when the last batch was released, and then creating N_ε new energy particles. To keep track of such increments, we maintain at each component a quantized version of energy, say $\tilde{W}_{\mathcal{C}}$, which is always a multiple of $\varepsilon N_\varepsilon$. Whenever a batch is released, we increment $\tilde{W}_{\mathcal{C}}$ by $\varepsilon N_\varepsilon$. Whenever $W_{\mathcal{C}}$ drops by about $\varepsilon N_\varepsilon$, we decrement $\tilde{W}_{\mathcal{C}}$ by $\varepsilon N_\varepsilon$ (this, we assume, is accompanied by the destruction of N_ε particles, something we don't necessarily monitor). As for the placement of the N_ε particles, we space them uniformly at the centers of N_ε equal adjacent partitions of the $\Delta\theta_{\mathcal{C}}$ arc, in view of the uniformity of energy production over the component extent, as we remarked above.

4.2.3 Initialization of the Particle System

It is possible to start the flow visualization using no initially placed particles, which is equivalent to ignoring the initial energy transfers until the first batch of particles is released. However, it is often desirable to initialize the system of particles, in such a way that the distribution is consistent with the initial energy density.

A simple initialization scheme is to uniformly place N_{init} particles, where $N_{\text{init}} = \left(\int_0^{2\pi}\int_0^a u(r,\theta)r\mathrm{d}r\mathrm{d}\theta\right)/\varepsilon$. Although there is no unique definition of "uniform placement", when $u(r,\theta)$ is indeed uniform, e.g. an LC circuit with an initially charged inductor and discharged capacitor, this is the best we expect to do. When that is not the case, this is still a simple initialization that one can adopt. Instead of uniform placement, it is also possible to have random placement of the N_{init} particles.

In the more general case, one solution we considered is to place particles by pre-evolving the system in a steady state exactly equal to the initial state of the circuit. For example, an RC circuit with a battery and an initially discharged capacitor has a resistor-battery type initial state. By evolving that state starting with no particles, the battery releases several batches of particles until they permeate the entire area, at which point (say when the first batch of particles is absorbed by the resistor) the pre-evolution is stopped, and the actual simulation is started.

Chapter 5

Conclusion

5.1 Examples

We conclude with three examples: an RC circuit with a battery switched on and off, an LC oscillator circuit, and a two-resistor circuit with a battery. Through these examples, we both illustrate the development of this thesis and convey some final remarks concerning the rough edges remaining for future investigation. In what follows, the characteristic colors $\mathbf{C_E}$ and $\mathbf{C_B}$ for the electric and magnetic fields are light gray and black respectively.

RC Circuit

Fig. 5-1 illustrates the energy flow in an RC circuit[1]. In the first row, a battery is initially connected, and the capacitor charges up: notice how the energy flow is gradually deflected from the resistor to the capacitor. Once the capacitor is half charged, we remove the battery, thus connecting the capacitor directly to the resistor. The outcome is depicted in the second row. Note that the existing particles at this point no longer reflect the true energy density, since the electric field due to the battery has been removed. After the short transient, these overflow particles are eliminated, and energy then flows from the capacitor to the resistor in batches.

[1] Circuit diagrams are overlaid manually on the simulation.

We can complement this experiment with various measurements, such as particle counts. We can show for example that, in the charging scenario, the energy released by the battery is always divided evenly between dissipation in the resistor and absorption by the capacitor, regardless of component values. Fig. 5-2 is a texture representation of the electric field when the capacitor is half charged, which explains the symmetry. The texture is generated by *integrating* streamlines at randomized positions, and then *drawing* them on an empty canvas using a randomized color [12].

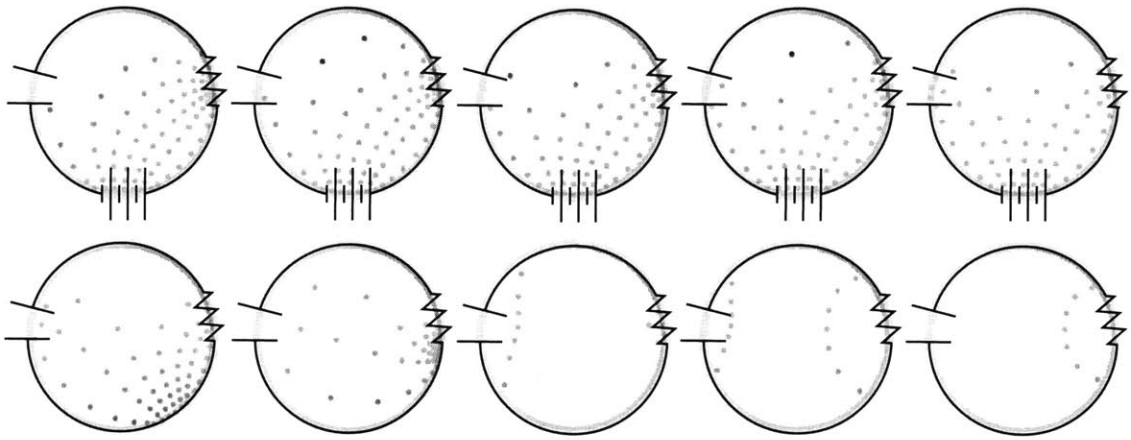

Figure 5-1: RC Circuit: Energy flow for a charging capacitor (top), which then discharges (bottom) through the resistor, once the battery is removed.

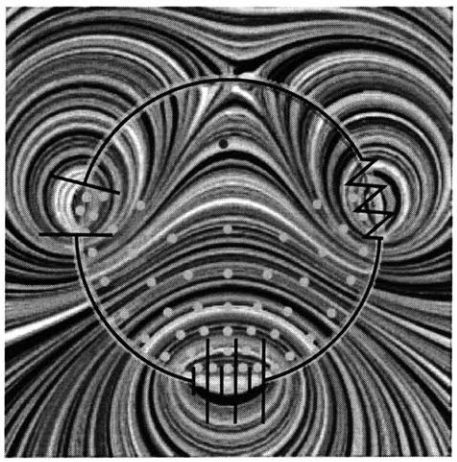

Figure 5-2: RC Circuit: Circuit electric field when the capacitor is half charged, and the battery is still in the circuit.

LC Oscillator

Fig. 5-3 illustrates the energy flow in an LC oscillator, with an initially charged inductor and a discharged capacitor. As we remarked in Sec. 4.2.3, we start with a uniform distribution. The alternation between electric and magnetic energy is evident: initially all energy is magnetic (black), but when the capacitor is fully charged it becomes entirely electric (light gray). The mismatch of spacing between the energy particles flowing out of the capacitor, as compared to the initial configuration, is due to the fact that we initialize particles on a lattice, whereas the released batches are placed on the arc corresponding to the capacitor and then propagate. However, the number of particles and overall coverage of the cylinder's interior is still the same.

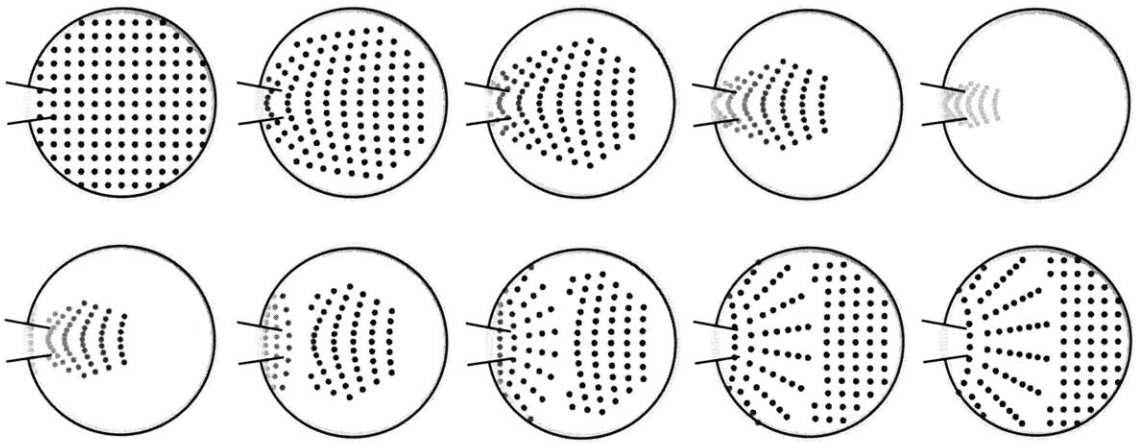

Figure 5-3: LC Oscillator: Energy flow with an initial current in the inductor and an initially discharged capacitor. The capacitor fully charges (top), then discharges (bottom) and the cycle restarts.

It is worth remarking that since neglecting the displacement current is not a good approximation near the capacitor in this case, an excess of energy particles are absorbed by the capacitor. Therefore, when re-releasing energy, we release a certain fraction more than what we've obtained in Chap. 4, to compensate. This issue is worth investigating in the future. Fig. 5-4 illustrates the electric field of the circuit when the capacitor carries some charge.

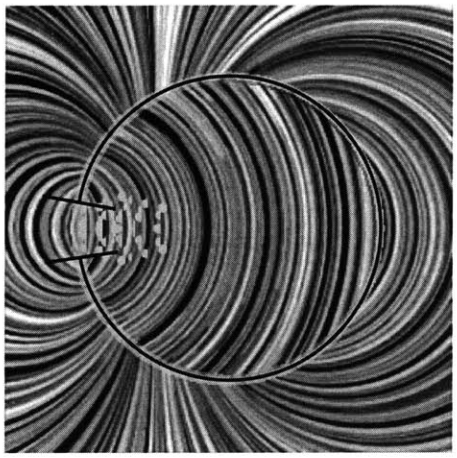

Figure 5-4: LC Oscillator: Circuit electric field when the capacitor carries some charge. Only the field magnitude is affected by charge, not the depicted direction.

Two Resistors

Fig. 5-5 and Fig. 5-6 illustrate two configurations with one battery and two resistors. We only give a snapshot of the energy flow, as this is a steady-state situation, and the directions of flow do not change. In Fig. 5-5 both resistors have equal resistance, whereas in Fig. 5-6 the resistance of the left resistor is twice that of the right one, but their sum is kept the same. Naturally, everything is symmetric in the first case. For the second case, notice how the resistor with the larger resistance dissipates twice as much energy, as evidenced by twice as many energy particle streams flowing into it.

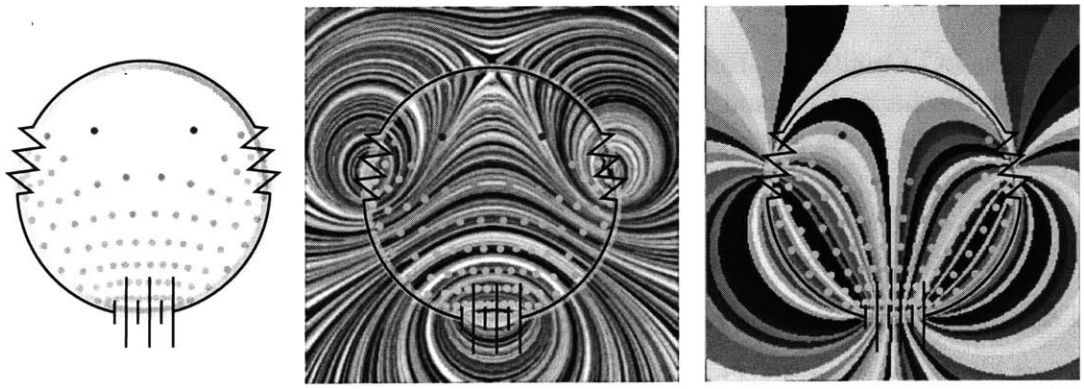

Figure 5-5: Two Resistors: Energy flow (left), electric field (middle), and electrostatic potential isocontours (right). Both resistances are equal.

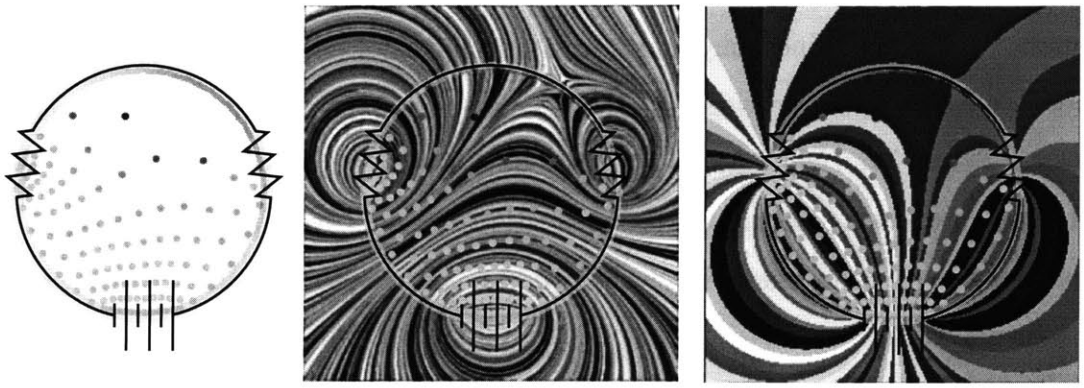

Figure 5-6: Two Resistors: Energy flow (left), electric field (middle), and electrostatic potential isocontours (right). The left resistance is twice the right resistance, with the sum the same as that in Fig. 5-5.

In Fig. 5-5 and Fig. 5-6, we also show the electric field, together with the isocontours of the electrostatic potential. The isocontours texture is efficiently generated by first computing an image of the potential, by following Chap. 3, and then randomizing the color map used to display it. This scheme has not been published previously. It allows one not only to visualize the isocontours, but also to efficiently generate a texture representation of any vector field that can be written as normal to the gradient of a scalar field.

The reason why we want to see the isocontours is to observe that, in the electrostatic case, energy flows along them, since both these and the Poynting vector are normal to the electric field everywhere. This is not true in the general case, since while the Poynting vector continues to be normal to the total electric field, the scalar potential's isocontour becomes normal only to the curl-free component.

5.2 Summary

To summarize, in this thesis we addressed the problem of simulating and visualizing electric and magnetic fields and energy flows in electric circuits with idealized geometries. Our motivation was primarily educational: to bridge the gap between the teaching of electricity and magnetism and that of electric circuits.

To simplify analysis and computation, we adopted an infinite-height cylindrical geometry. We then defined physical properties that allowed us to specify a spectrum of possible circuit configurations. With these, we obtained expressions for the electromagnetic fields. We then described energy flow in this circuit as a function of these fields, and proposed a meaningful visualization thereof. Finally, we illustrated our development with some examples, which we also used to indicate areas where we plan to do future work.

What remains is to adapt our tool to the curriculum of introductory physics courses, by making it part of both qualitative and quantitative exercises. We believe that by experimenting with these simulations and visualizations after covering basic electromagnetism, students will become more aware of the physical nature of electric circuits.

Bibliography

[1] Brian Cabral and Leith Casey Leedom. Imaging vector fields using line integral convolution. In D. Bartz, editor, *20th Annual Conference on Computer Graphics and Interactive Techniques*, pages 263–270. ACM, SIGGRAPH, August 1993.

[2] George W. Clark. Note on the electric field around a cylindrical inductor. Private communication to John W. Belcher., 2004.

[3] James W. Cooley and John W. Tukey. An algorithm for the machine computation of complex Fourier series. *Mathematics of Computation*, 19:297–301, 1965.

[4] Carl F. Gauss. Nachlass: Theoria interpolationis methodo novo tractata. In *Carl Friedrich Gauss, Werke, Band 3*, pages 265–303. Königliche Gesellschaft der Wissenschaften zu Göttingen, 1866.

[5] David J. Griffiths. *Introduction to Electrodynamics.* Prentice Hall, Upper Saddle River, New Jersey, third edition, 1999.

[6] Mark A. Heald. Electric fields and charges in elementary circuits. *American Journal of Physics*, 52(6):522–526, June 1984.

[7] Mark A. Heald. Energy flow in circuits with Faraday emf. *American Journal of Physics*, 56(6):540–547, June 1988.

[8] In *The Codex of Ultimate Wisdom*, page 1. Unknown Origin, Unknown Era.

[9] John D. Jackson. Surface charges on circuit wires and resistors play three roles. *American Journal of Physics*, 64(7):855–870, July 1996.

[10] John D. Jackson. *Classical Electrodynamics.* John Wiley and Sons, New York, third edition, 1999.

[11] Slavko Majcen, Ryan K. Haaland, and Scott C. Dudley. The Poynting vector and power in a simple circuit. *American Journal of Physics*, 68(9):857–859, January 2000.

[12] Carlos Pérez Risquet. Visualizing 2D flows: Integrate and Draw. In *9th Eurographics Workshop on Visualization in Scientific Computing*, pages 132–142, April 1998.